

Maintenance of murine platelet homeostasis by the kinase Csk and phosphatase CD148

Citation for published version (APA):

Mori, J., Nagy, Z., Di Nunzio, G., Smith, C. W., Geer, M. J., Al Ghaithi, R., van Geffen, J. P., Heising, S., Boothman, L., Tullemans, B. M. E., Correia, J. N., Tee, L., Kuijpers, M. J. E., Harrison, P., Heemskerk, J. W. M., Jarvis, G. E., Tarakhovsky, A., Weiss, A., Mazharian, A., & Senis, Y. A. (2018). Maintenance of murine platelet homeostasis by the kinase Csk and phosphatase CD148. *Blood*, 131(10), 1122-1144. <https://doi.org/10.1182/blood-2017-02-768077>

Document status and date:

Published: 08/03/2018

DOI:

[10.1182/blood-2017-02-768077](https://doi.org/10.1182/blood-2017-02-768077)

Document Version:

Publisher's PDF, also known as Version of record

Document license:

Taverne

Please check the document version of this publication:

- A submitted manuscript is the version of the article upon submission and before peer-review. There can be important differences between the submitted version and the official published version of record. People interested in the research are advised to contact the author for the final version of the publication, or visit the DOI to the publisher's website.
- The final author version and the galley proof are versions of the publication after peer review.
- The final published version features the final layout of the paper including the volume, issue and page numbers.

[Link to publication](#)

General rights

Copyright and moral rights for the publications made accessible in the public portal are retained by the authors and/or other copyright owners and it is a condition of accessing publications that users recognise and abide by the legal requirements associated with these rights.

- Users may download and print one copy of any publication from the public portal for the purpose of private study or research.
- You may not further distribute the material or use it for any profit-making activity or commercial gain
- You may freely distribute the URL identifying the publication in the public portal.

If the publication is distributed under the terms of Article 25fa of the Dutch Copyright Act, indicated by the "Taverne" license above, please follow below link for the End User Agreement:

www.umlib.nl/taverne-license

Take down policy

If you believe that this document breaches copyright please contact us at:

repository@maastrichtuniversity.nl

providing details and we will investigate your claim.

THROMBOSIS AND HEMOSTASIS

Maintenance of murine platelet homeostasis by the kinase Csk and phosphatase CD148

Jun Mori,^{1,*} Zoltan Nagy,^{1,*} Giada Di Nunzio,¹ Christopher W. Smith,¹ Mitchell J. Geer,¹ Rashid Al Ghaithi,² Johanna P. van Geffen,³ Silke Heising,¹ Luke Boothman,¹ Bibian M. E. Tullemans,³ Joao N. Correia,¹ Louise Tee,¹ Marijke J. E. Kuijpers,³ Paul Harrison,² Johan W. M. Heemskerk,³ Gavin E. Jarvis,⁴ Alexander Tarakhovsky,⁵ Arthur Weiss,⁶ Alexandra Mazharian,¹ and Yotis A. Senis¹

¹Institute of Cardiovascular Sciences and ²Institute of Inflammation and Ageing, College of Medical and Dental Sciences, University of Birmingham, Birmingham, United Kingdom; ³Department of Biochemistry, Cardiovascular Research Institute Maastricht, Maastricht University, Maastricht, The Netherlands; ⁴Department of Physiology, Development and Neuroscience, University of Cambridge, Cambridge, United Kingdom; ⁵Laboratory of Immune Cell Epigenetics and Signaling, The Rockefeller University, New York, NY; and ⁶Department of Medicine, Rosalind Russell-Ephraim P. Engleman Rheumatology Research Center and Howard Hughes Medical Institute, University of California, San Francisco, San Francisco, CA

KEY POINTS

- Csk and CD148 are nonredundant regulators of SFKs in platelets, and deletion of either induces cell-intrinsic negative feedback mechanisms.
- Csk is a negative regulator of SFK activity, whereas CD148 is a dual positive and negative regulator of SFK activity in platelets.

Src family kinases (SFKs) coordinate the initiating and propagating activation signals in platelets, but it remains unclear how they are regulated. Here, we show that ablation of C-terminal Src kinase (Csk) and receptor-like protein tyrosine-phosphatase CD148 in mice results in a dramatic increase in platelet SFK activity, demonstrating that these proteins are essential regulators of platelet reactivity. Paradoxically, Csk/CD148-deficient mice exhibit reduced in vivo and ex vivo thrombus formation and increased bleeding following injury rather than a prothrombotic phenotype. This is a consequence of multiple negative feedback mechanisms, including downregulation of the immunoreceptor tyrosine-based activation motif (ITAM)- and hemi-ITAM-containing receptors glycoprotein VI (GPVI)-Fc receptor (FcR) γ -chain and CLEC-2, respectively and upregulation of the immunoreceptor tyrosine-based inhibition motif (ITIM)-containing receptor G6b-B and its interaction with the tyrosine phosphatases Shp1 and Shp2. Results from an analog-sensitive Csk mouse model demonstrate the unconventional role of SFKs in activating

ITIM signaling. This study establishes Csk and CD148 as critical molecular switches controlling the thrombotic and hemostatic capacity of platelets and reveals cell-intrinsic mechanisms that prevent pathological thrombosis from occurring. (Blood. 2018;131(10):1122-1144)

Introduction

Platelets are highly reactive fragments of megakaryocytes (MKs) that interrogate the vessel wall and prevent excessive blood loss following injury. They do so by adhering to exposed extracellular matrix proteins and forming a thrombus that transiently occludes the blood vessel, promoting wound repair and vessel regeneration. However, it remains unclear how the reactivity of platelets in the circulation is regulated.

Platelets contain high levels of Src family kinases (SFKs) that have a coordinating role in initiating and propagating primary activation signals.^{1,2} The 3 most abundant SFKs in human and mouse platelets are Src, Lyn, and Fyn (supplemental Figure 1, available on the Blood Web site).^{3,4} Src and Fyn act primarily as positive regulators of platelet activation,⁵⁻⁸ whereas Lyn is both a positive and negative regulator of activation.^{9,10} SFKs are constitutively associated with the cytoplasmic tails of several important platelet receptors, including the glycoprotein Ib (GPIb)-IX-V complex,^{11,12} the immunoreceptor tyrosine-based activation motif (ITAM)-containing GPVI-Fc receptor (FcR) γ -chain receptor complex,^{5,13}

and the integrin α IIb β 3.^{14,15} SFKs are also involved in transmitting secondary activation signals from G protein-coupled receptors.¹⁶⁻²¹

Equally important, but less well understood are the inhibitory functions of SFKs. Concomitant with phosphorylating ITAM-containing receptors activating platelets,^{5,22} SFKs also phosphorylate immunoreceptor tyrosine-based inhibition motif (ITIM)-containing receptors that inhibit platelets.²³ The latter recruit SH2 domain-containing phosphatases, including the nontransmembrane protein-tyrosine phosphatases Shp1 and Shp2,²⁴⁻²⁶ that inhibit platelet activation. The 2 most well-characterized platelet ITIM-containing receptors are PECAM-1 and G6b-B, which inhibit platelet activation and modulate platelet homeostasis, respectively.^{27,28}

Limited knowledge has been gained about how platelet SFKs are regulated. SFKs are primed by dephosphorylation of the C-terminal inhibitory phosphotyrosine residue by the receptor-like tyrosine phosphatase CD45 in most hematopoietic cells²⁹ and by CD148 in platelets.³⁰⁻³² Primed SFKs need to be fully

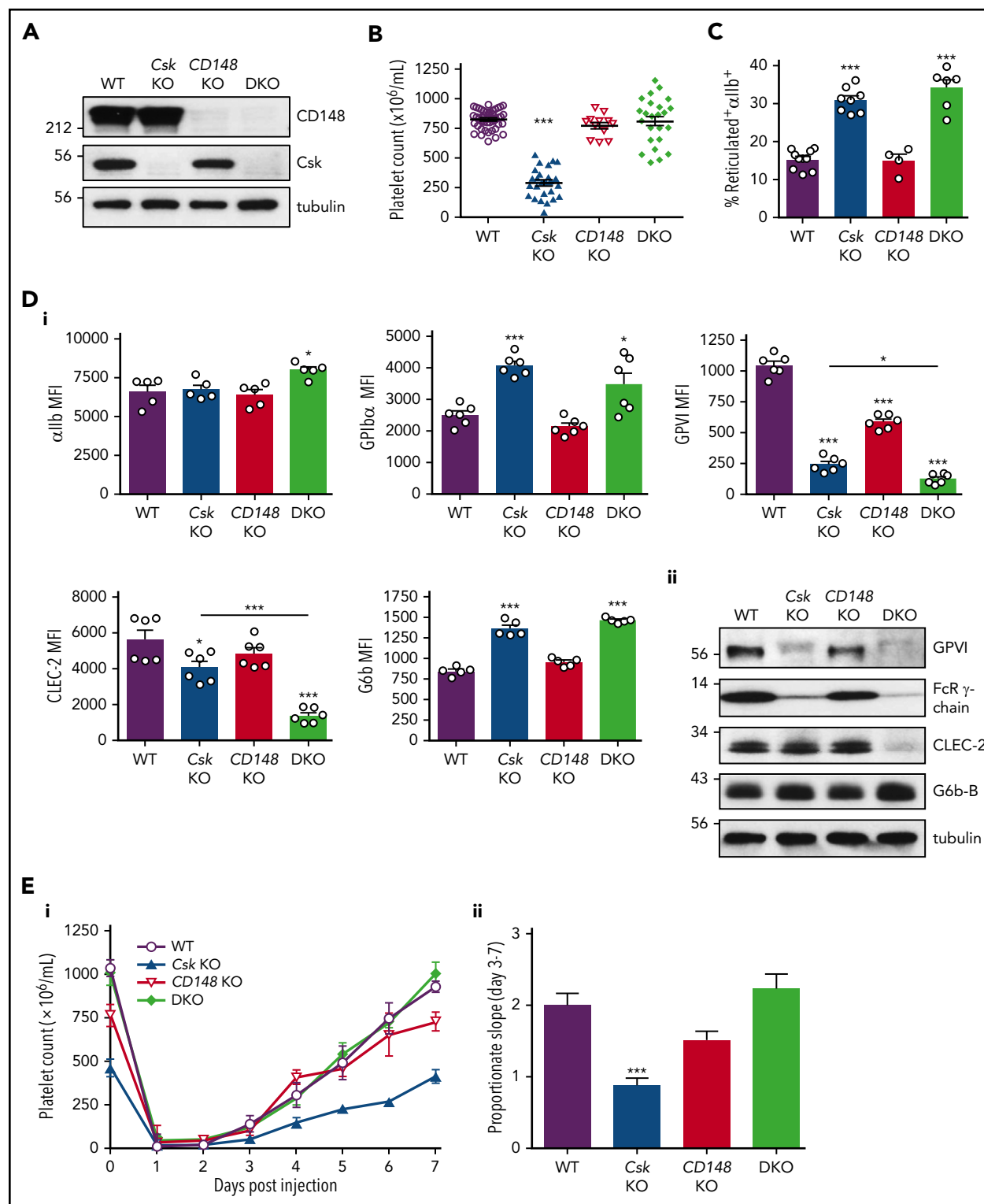


Figure 1. Aberrant platelet production and platelet receptor expressions in Csk KO mice. (A) Platelet lysates were blotted for the indicated proteins. (B) Platelet counts. (C) Percentage of reticulated platelets determined by thiazole orange $^+$ αIIb^+ cells in blood. See also supplemental Figure 2A. (Di) Median fluorescence intensity (MFI) measured in αIIb^+ cells alone or αIIb^+ cells costained for the indicated proteins in blood ($n = 5$ –6 mice per genotype). See also supplemental Figure 3. (Dii) Platelet lysates were blotted for the indicated proteins. (Ei) Platelet counts of pre-/postinjection of anti-GPIIb antibody (1.5 $\mu\text{g}/\text{g}$ body weight). (Eii) The rate of platelet recovery determined by a proportionate slope from linear trend lines between days 3 and 7 from panel Ei ($n = 7$ –8 mice per genotype). See also supplemental Figures 4–6. Asterisks refer to significant difference compared with WT (* $P < .05$, *** $P < .001$; 1-way ANOVA with Tukey's test in B–D or 1-way ANOVA with Dunnett's test; vs WT in E); data represent mean \pm SEM.

activated through *trans*-autophosphorylation of a tyrosine residue located within the catalytic domain.³³ On the other hand, inactivation of SFKs can occur through the action of C-terminal

Src kinase (Csk) and the structurally related Csk homologous kinase (Chk), also referred to as megakaryocyte-associated tyrosine kinase (Matk), both of which target the C-terminal inhibitory tyrosine

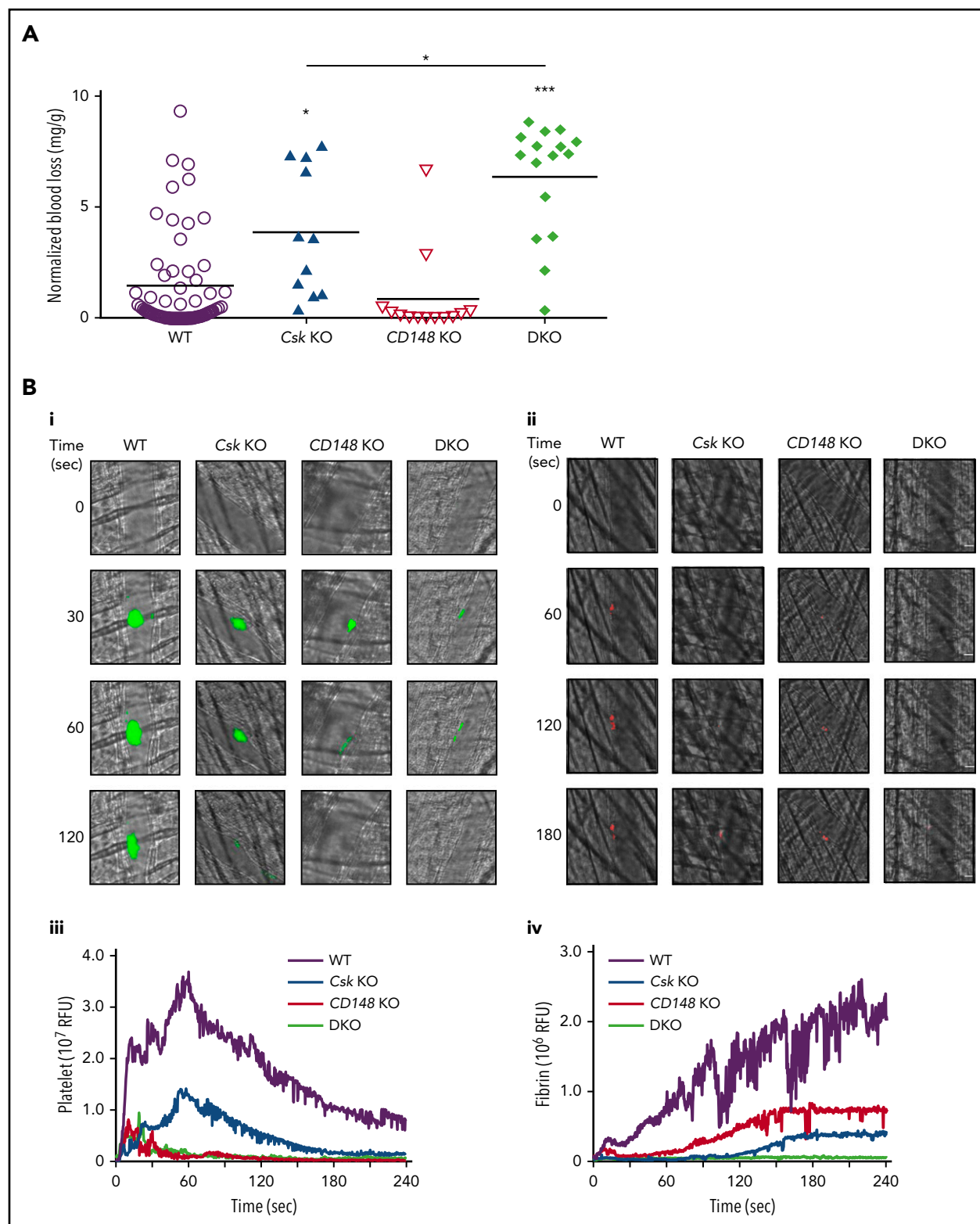


Figure 2. Increased bleeding and defective thrombus formation in *Csk* KO and DKO mice. (A) Hemostatic response was measured in tail bleeding assays by an excision of a 5-mm portion of the tail tip followed by the determination of lost blood/body weight (normalized blood loss) ($n = 11$ –57 mice per genotype). Tail bleeding assays were conducted in a double-blinded manner. (B) Laser injury–induced thrombus formation in vivo. Composite bright-field and fluorescence images of (Bi) platelet accumulation (green) or (Bii) fibrin generation (red) in cremaster muscle arterioles monitored by DyLight488-labeled anti-GPIIb/IIIa antibody (0.1 μ g/g body weight) or Alexa Fluor 647–labeled anti-fibrin antibody (0.2 μ g/g body weight) signal, respectively by confocal intravital microscopy (scale bar, 10 μ m). Each curve represents the median integrated fluorescence intensity of (Biii) platelets or (Biv) fibrin in relative fluorescence units (RFUs) ($n = 25$ –37; 5 mice per genotype). See also supplemental Videos 1 and 2. (C) FeCl_3 injury–induced thrombus formation in vivo. Filter paper soaked in 10% FeCl_3 was applied to carotid artery for 3 minutes. (Ci) Representative fluorescence images of platelet accumulation (green) monitored by DyLight488-labeled anti-GPIIb/IIIa antibody (0.1 μ g/g body weight) by confocal intravital microscopy (scale bar, 200 μ m). (Cii) Each curve represents the median integrated thrombus fluorescence intensity in RFU. (Ciii) Area under the curve (AUC) was measured ($n = 8$ –11 mice per genotype). See also supplemental Video 3. * $P < .05$, ** $P < .01$, *** $P < .001$; 1-way ANOVA with Tukey's test; data represent mean \pm SEM.

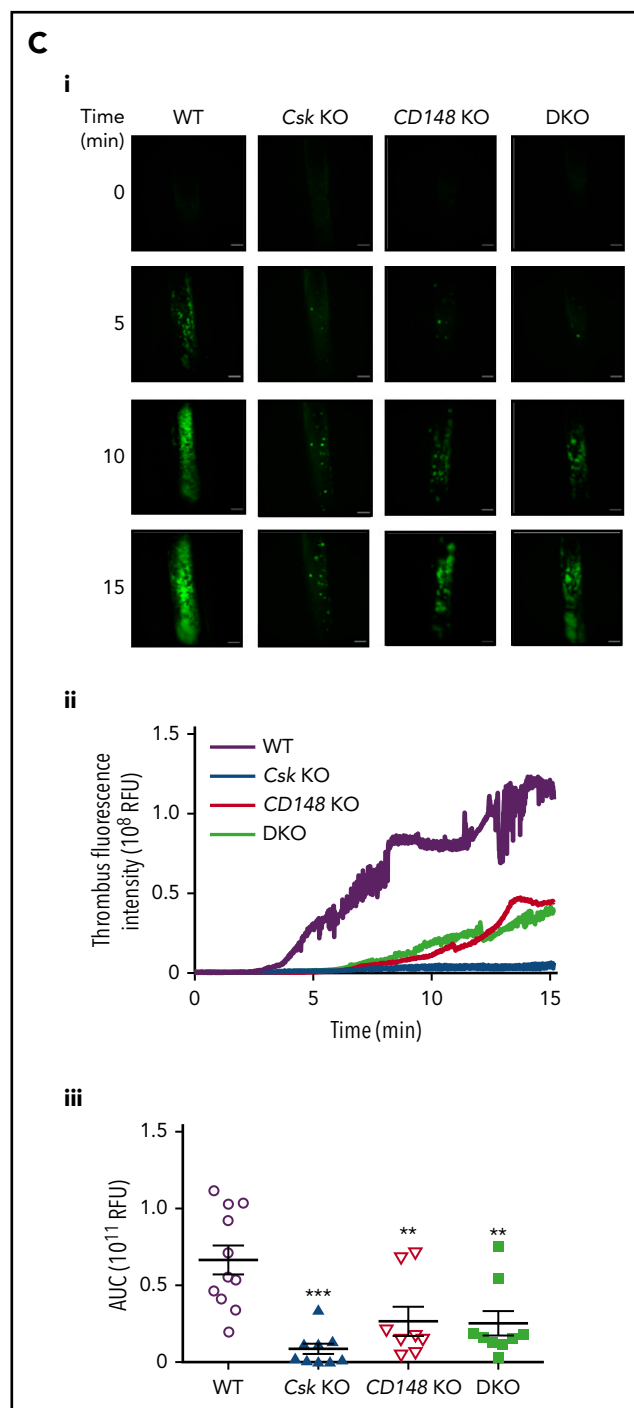


Figure 2. (Continued).

residue in SFKs.^{34,35} However, it remains unknown how the threshold of individual SFK activation is set in platelets

To address these questions, we generated a series of MK-specific conditional knockout (KO) mouse models leading to deletion of *Csk*, *CD148*, or *Csk/CD148* and studied the consequences of these deletions for platelet physiology. Disruption of the homeostatic balance of SFK activity in MKs had dramatic and unexpected consequences on the number and reactivity of platelets in the circulation due to cell-intrinsic negative feedback

mechanisms involving the ITIM-containing receptor G6b-B and Chk, culminating in antithrombotic and hemorrhagic outcomes.

Materials and methods

Mice

Csk^{fl/fl}, *CD148^{fl/fl}*, *Pf4-Cre⁺*, and *Csk^{ΔS}* mice were generated as previously described.³⁶⁻³⁹ All mice were on a C57BL/6 background. All procedures were undertaken with United Kingdom Home Office approval in accordance with the Animals (Scientific Procedures) Act of 1986.

Antibodies and reagents

Thiazole orange (BD Retic-Count) was from BD Biosciences. PP1 analog IV (3-IB-PP1) was from Calbiochem. Antibodies are described in detail in supplemental Methods.

Immune thrombocytopenia

Thrombocytopenia was induced as previously described.²⁸

Platelet preparation

Blood was collected from terminally CO₂-narcosed mice from the abdominal vena cava into 1:10 (v/v) acid-citrate-dextrose anticoagulant. Washed platelets were prepared as previously described.⁴⁰ Adenosine diphosphate (ADP)-sensitive washed platelets were prepared in the presence of ADP scavenger apyrase as previously described.⁴¹ Platelet counts were normalized and used for spreading (2×10^7 /mL), aggregation (2×10^8 /mL), or biochemical analysis ($4-5 \times 10^8$ /mL).

Platelet functional assays and biochemistry

Platelet aggregation, adenosine triphosphate (ATP) secretion, spreading, clot retraction, platelet adhesion under flow, total thrombus formation analysis system (T-TAS), stimulation for biochemical analysis, immunoblotting, and immunoprecipitation are described in detail in the supplemental Methods.

Flow cytometry

Reticulated platelets in blood were double stained with α IIb and thiazole orange (BD Retic-Count; BD Biosciences). Surface protein expression was measured in blood or bone marrow cells with indicated FITC- or PE-conjugated antibodies by flow cytometry (BD Accuri C6 for platelets; BD FACSCalibur for bone marrow cells), as previously described.^{25,28}

Tail bleeding assay

Experiments were performed on 8- to 10-week-old KO and litter-matched wild-type (WT) mice as previously described.³⁰

In vivo thrombosis assays

Laser-induced injury of arterioles in the cremaster muscle and ferric chloride (FeCl₃)-induced injury of carotid arteries were performed and analyzed as previously described.⁴²

Statistical analysis

Data presented are mean \pm standard error of the mean (SEM). One-way or 2-way analysis of variance (ANOVA) followed by post-hoc tests were used to determine statistical significance ($P < .05$). Further details on statistical analysis are provided in the supplemental Methods.

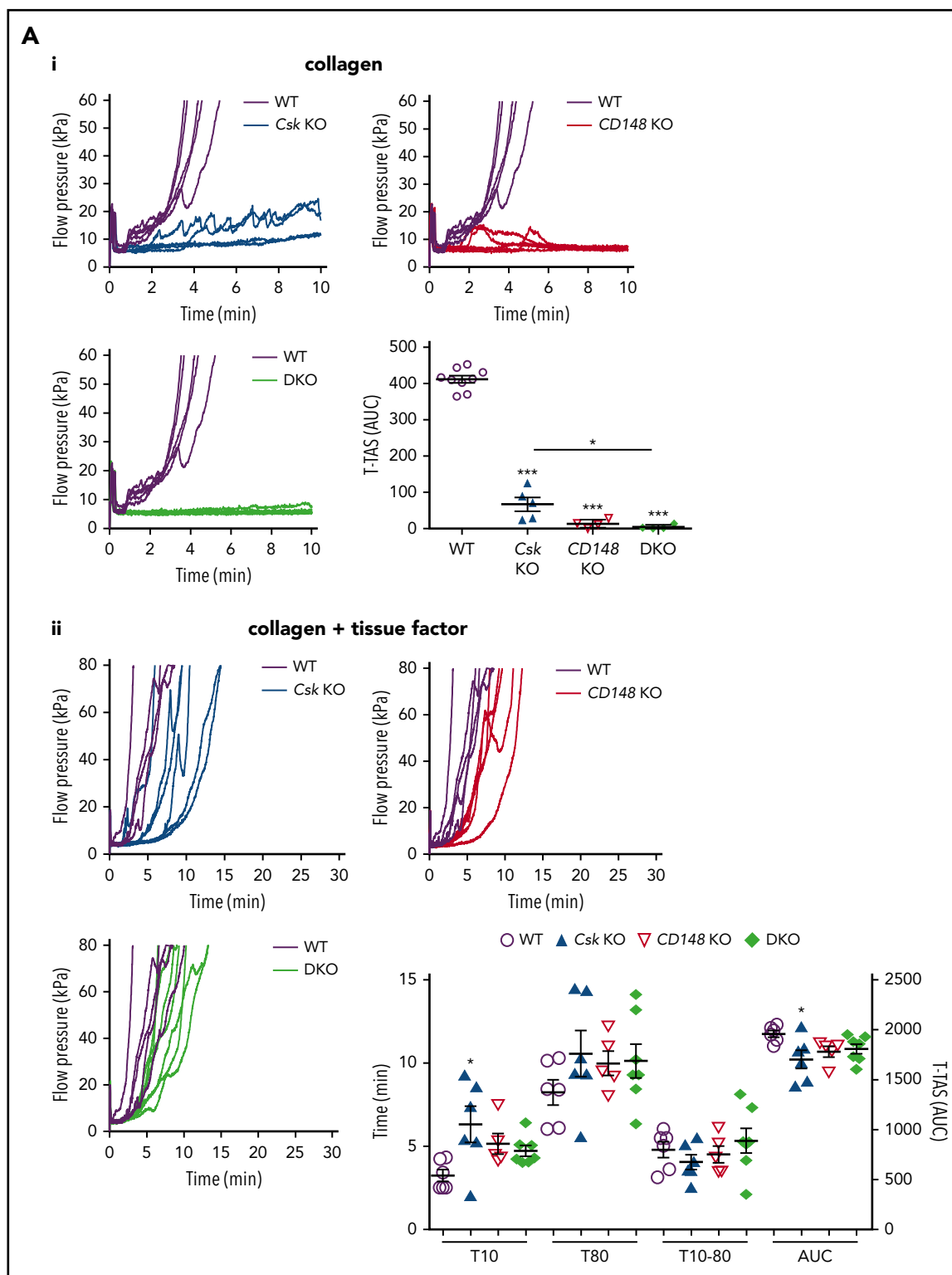


Figure 3. Aberrant platelet functions in *Csk* KO, *CD148* KO, and *DKO* mice. (Ai) 25 μ g/mL hirudin-treated blood was perfused with collagen-coated chip at 1000 s^{-1} for 10 minutes. Individual time-dependent flow pressure curves and total thrombogenicity (area under the curve [AUC]) were measured by the total thrombus-formation analysis system (T-TAS). (Aii) Blood treated with 3.2% sodium citrate, 12 mM $CaCl_2$, and 50 μ g/mL corn trypsin inhibitor was perfused on collagen plus tissue thromboplastin (tissue factor)-coated chip at 240 s^{-1} for 30 minutes. Individual time-dependent flow pressure curves, time to onset (T10), time to occlusion (T80), rate of thrombus growth (T10-80), and AUC were measured by T-TAS ($n = 4-9$ per genotype). (B) Blood treated with 5 U/mL heparin, 40 μ M PPACK, and 50 U/mL Fragmin was perfused over microspots with indicated coatings; 100 μ g/mL collagen I, 12.5 μ g/mL vWF-BP, 50 μ g/mL laminin, and 250 μ g/mL rhodocytin for 3.5 minutes at 1000 s^{-1} . (Bi) Representative bright-field images with indicated surfaces. (Bii) Platelet deposition (percent surface area coverage [SAC]). (Biii) Multilayered thrombus (percent SAC) on the collagen I surface. (Biv) Representative fluorescence images of P-selectin, integrin α IIb β 3 activation (JON/A), and PS exposure (Annexin V) from the collagen surface, and (Bv) percent SAC of fluorescence images. (Bvi) Heatmap of outcome parameters expressed as effect sizes per genotype⁷⁶; P1, platelet deposition; P2, multilayered thrombus; P3, P-selectin; P4, JON/A; and P5, PS exposure from indicated surfaces. Scale bar represents 10 μ m. Experiments and analysis were performed in a double-blinded manner. Percent SAC was analyzed using Fiji ($n = 15$ images).

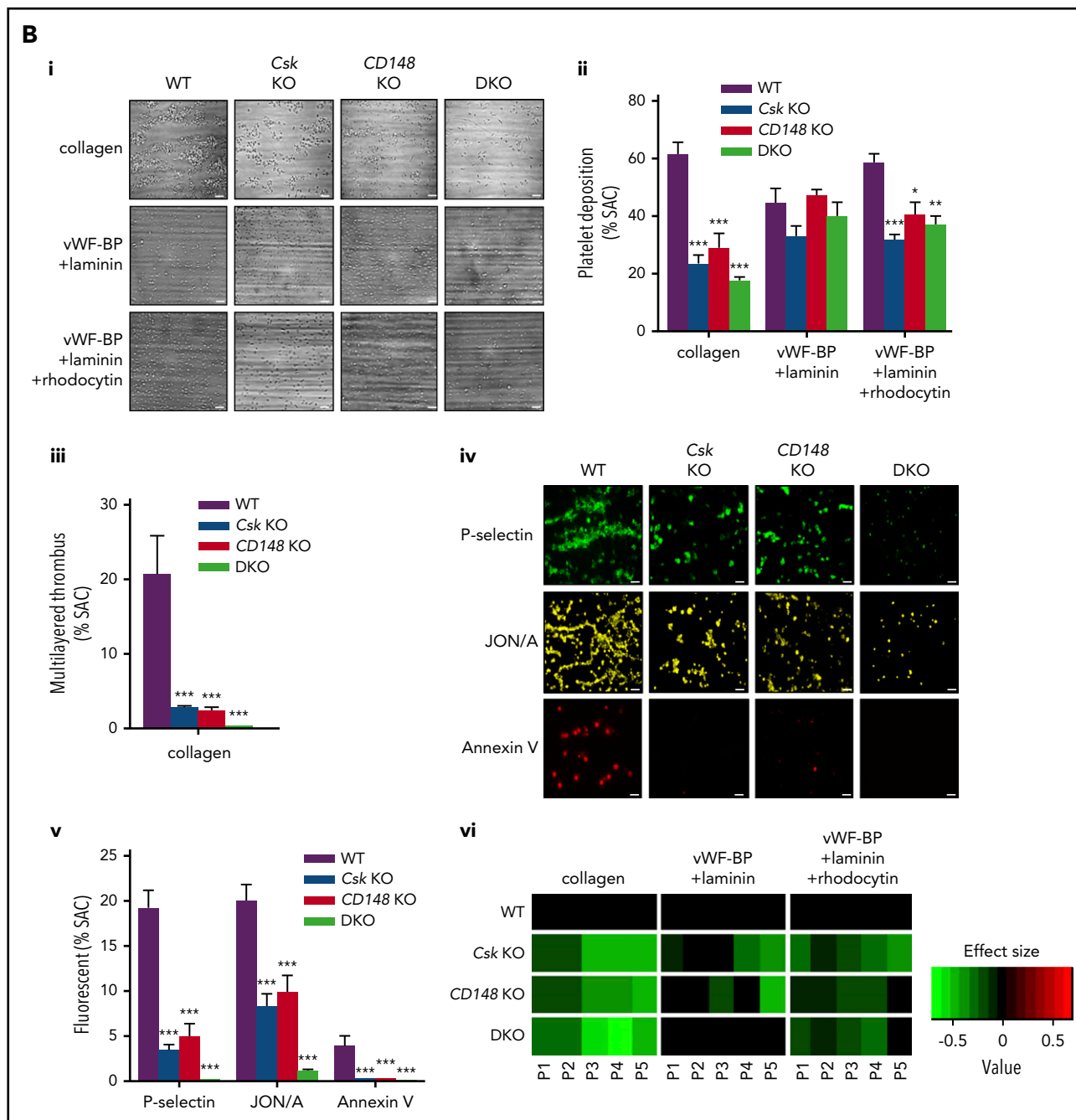


Figure 3. (Continued). from 5 mice per genotype). (C) Representative platelet aggregation and ATP secretion traces in response to the indicated agonists in (Ci-Cvi) washed platelets or (Cvii) ADP-sensitive washed platelets ($n = 4-8$ mice per condition per genotype). See also supplemental Figure 7. (Di) Representative differential interference contrast (DIC) microscopy images of resting (basal) and thrombin-stimulated (0.1 U/mL , 5 minutes) platelets spread on fibrinogen-coated coverslips ($100 \text{ } \mu\text{g/mL}$, 45 minutes, 37°C ; scale bar, $5 \text{ } \mu\text{m}$). (Dii) Mean surface area of individual platelets quantified by ImageJ ($n = 256$ platelets per condition per genotype). (E) Fibrin clot retraction was assessed 2 hours after the addition of 1 U/mL thrombin and 2 mM CaCl_2 to platelet-rich plasma. Clot volumes were expressed as a percentage of the initial volume of platelet-rich plasma ($n = 8$ per genotype). $*P < .05$, $**P < .01$, $***P < .001$; 2-way (Bii,Bv,D) or 1-way (A,Biii,E) ANOVA with Tukey's test; data represent mean \pm SEM.

Results

Rescue of thrombocytopenia in *Csk*/*CD148*-deficient mice

MK-specific *Csk* and *CD148* conditional KO (*Csk* and *CD148* KO) mice were generated by crossing *Csk*^{fl/fl} and *CD148*^{fl/fl} mice with *Pf4-Cre*⁺ transgenic mice, respectively.³⁶⁻³⁸ *Csk*/*CD148* conditional double KO (DKO) mice were also generated to determine

whether deletion of both enzymes simultaneously would rescue phenotypes of single KO mice and to reveal novel mechanisms of SFK regulation (Figure 1A).

Platelet count in *Csk* KO mice was reduced by 65% and platelet volume increased by 33% (Figure 1B; supplemental Table 1), suggesting defects in platelet production and/or clearance. This was supported by a twofold increase in the proportion of

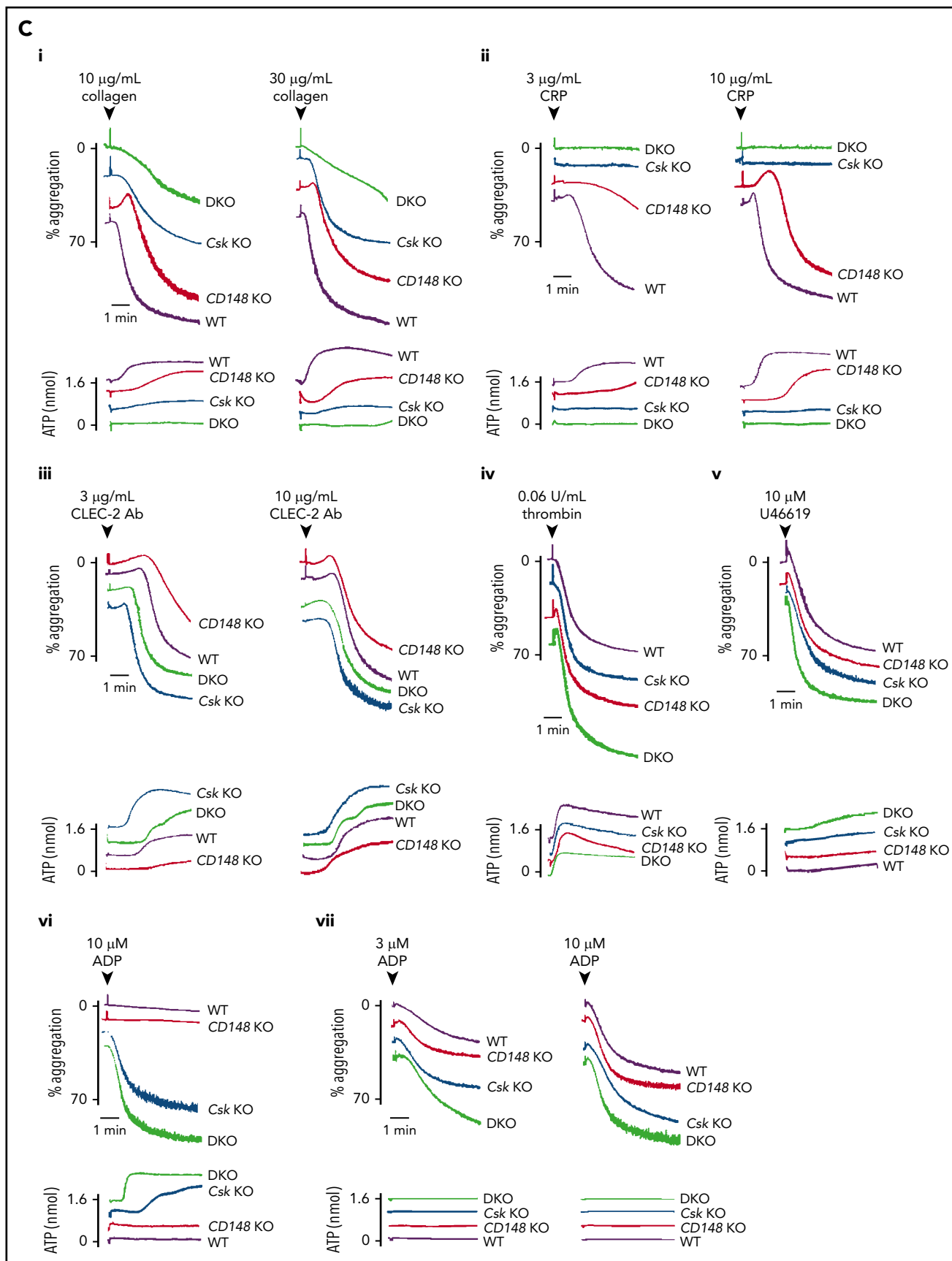
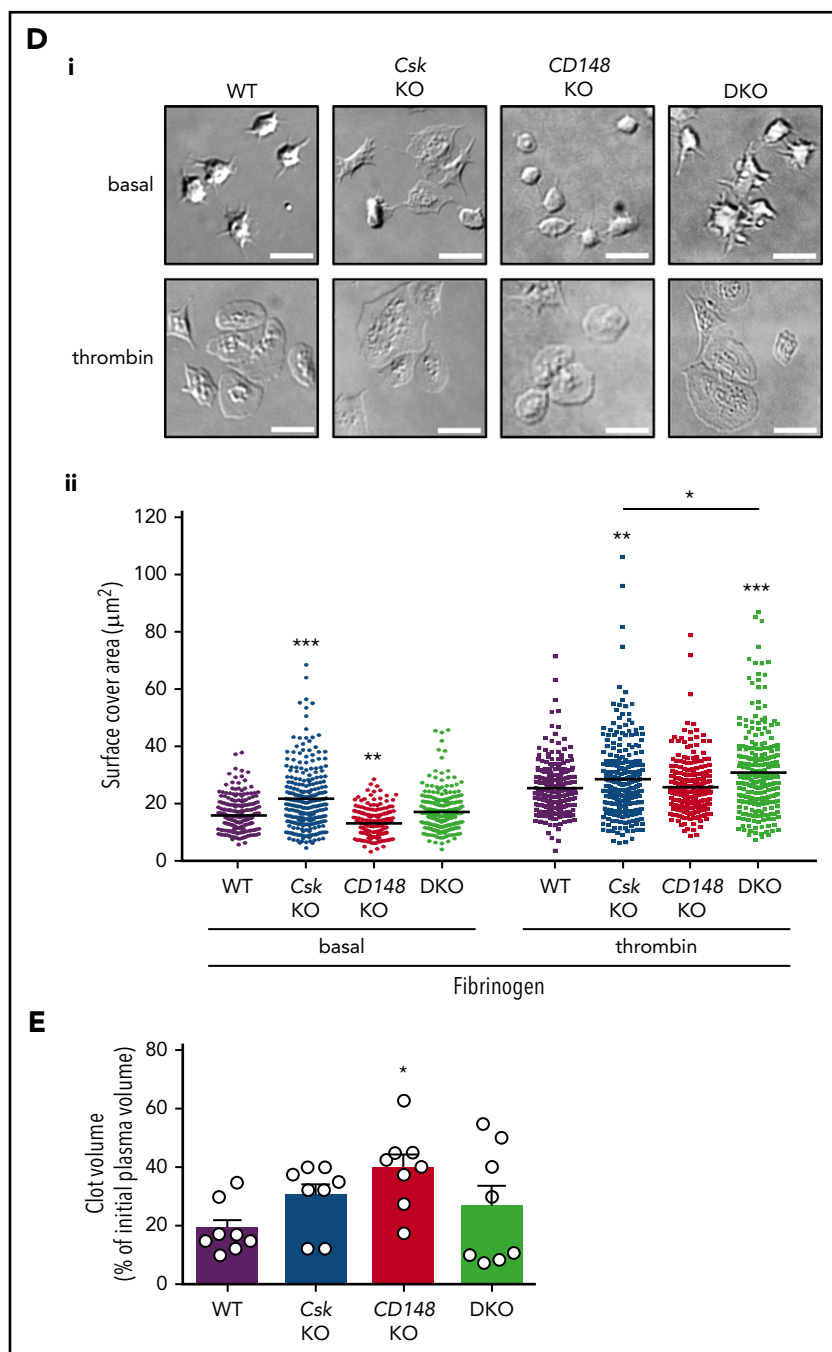


Figure 3. (Continued).

Figure 3. (Continued).



reticulated, immature platelets in these mice (Figure 1C; supplemental Figure 2A). The same parameters were normal in *CD148* KO mice (Figure 1B-C; supplemental Figure 2A). Although the platelet count was normal in DKO mice, the variability in numbers was greater than in WT and *Csk* KO mice, and the proportion of large, reticulated platelets was similar to that in *Csk* KO mice (Figure 1B-C; supplemental Figure 2A; supplemental Table 1). Increased numbers of immune and granulocytic cells in *Csk* and DKO mice (supplemental Table 1) may be an indirect consequence of nonspecific deletion of floxed *Csk* and *CD148* in other hematopoietic lineages by the *Pf4-Cre* transgene, which is reported to be "leaky."⁴³ Interestingly, the proportions of P-selectin⁺αIIb⁺ platelets were

normal in *Csk* KO mice and only marginally elevated in DKO mice (supplemental Figure 2B), pointing to only minimal preactivation of these platelets in the circulation or down-regulation of activation markers.

To explore whether increased platelet size and proportion of young platelets correlate with changes in other platelet parameters, we quantified levels of receptors that regulate platelet production and activation. Notably, several receptors we focused on, including αIIbβ3, GPIIbα, GPVI-FcR γ-chain, CLEC-2, and G6b-B, rely on SFKs to transmit signals.² Surface levels of integrin αIIb were marginally increased in DKO platelets, whereas GPIIbα levels were increased by 63% and

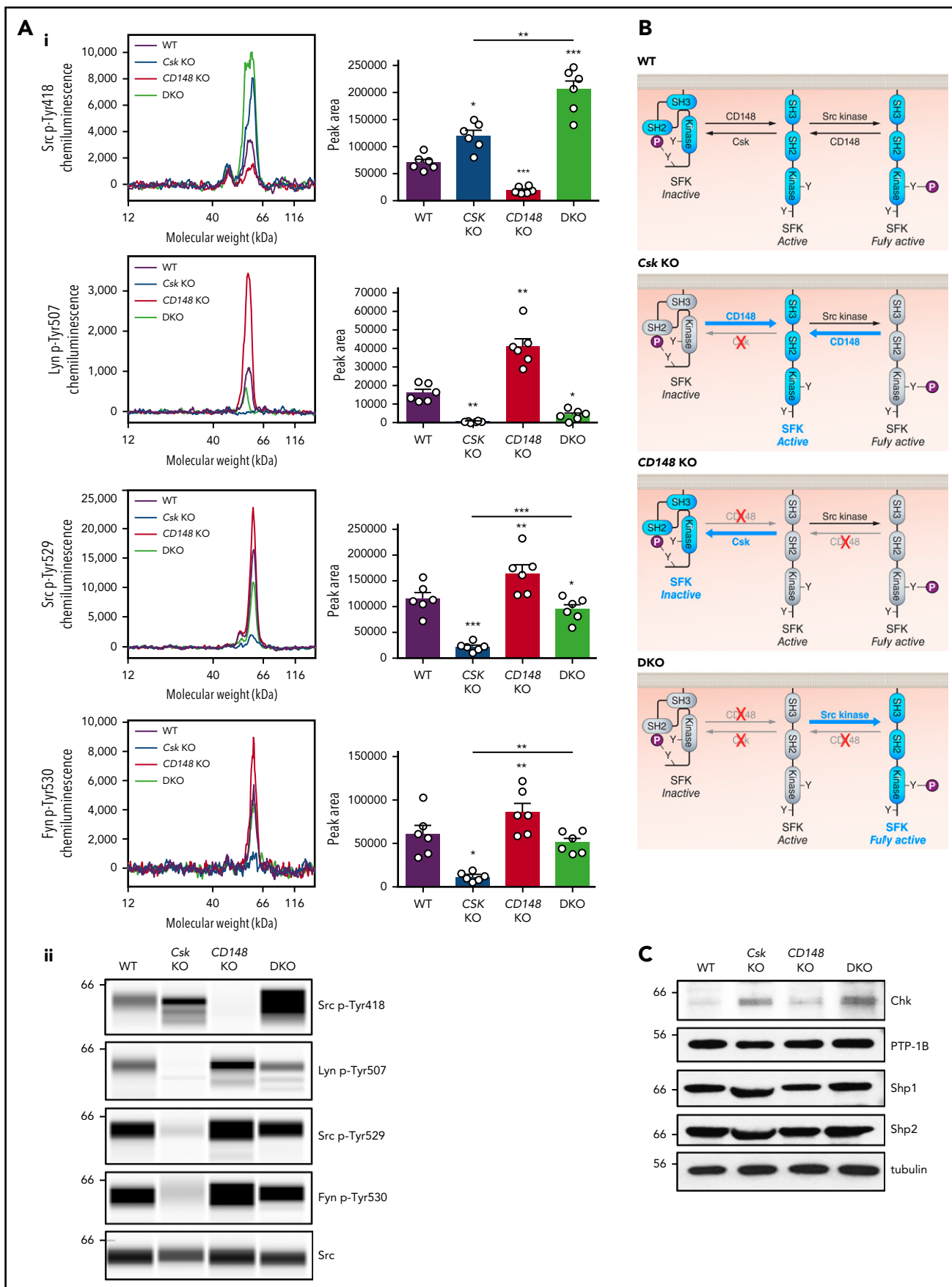


Figure 4.

38% in *Csk* KO and DKO platelets, respectively (Figure 1Di). Surface levels of GPVI were reduced by 77%, 44%, and 88% in *Csk* KO, *CD148* KO and DKO platelets, respectively, correlating with total protein levels of GPVI and FcR γ -chain (Figure 1Di-ii). Surface and total protein levels of CLEC-2 were reduced in *Csk* KO and DKO platelets, which were significantly more pronounced in DKO (Figure 1Di-ii). In contrast, surface expression of the inhibitory receptor G6b-B was increased by 61% and 73% in *Csk* KO and DKO platelets, respectively, correlating with total protein levels (Figure 1Di-ii). Surface levels of the integrin $\alpha 2$ subunit and metalloproteinase ADAM10 that mediates shedding of GPVI were normal (supplemental Figure 3A). Intriguingly, expression of surface receptors in αIIb^+ bone marrow cells was normal in all 3 genotypes (supplemental Figure 3B), suggesting autoregulation of these receptors in platelets. Collectively, these findings demonstrate down-regulation of the (hemi-)ITAM-containing activation receptors GPVI-FcR γ -chain and CLEC-2, and concomitant upregulation of the ITIM-containing inhibitory receptor G6b-B in *Csk*-deficient platelets.

To investigate the cause of low platelet counts, we measured the rate of platelet recovery following anti-GPIIb α antibody-mediated platelet depletion. This was significantly reduced in *Csk* KO mice, marginally reduced in *CD148* KO mice, and normal in DKO mice (Figure 1Ei-ii). The clearance of biotinylated platelets was normal in mice of all 3 genotypes (supplemental Figure 4A-B). Both *Csk* KO and DKO mice exhibited splenomegaly (supplemental Figure 5A-B). Elevated MK counts were observed in spleens in all 3 genotypes, which was associated with myelofibrosis (supplemental Figure 6A). MK counts were moderately elevated in the bone marrow of *Csk* KO mice, but with no associated myelofibrosis (supplemental Figure 6B). We observed more P-selectin $^+$ αIIb^+ hematopoietic cells in *Csk* KO and DKO mice (supplemental Figure 6C), which may explain the presence of myelofibrosis in the spleen of these mice.⁴⁴ Together, these findings suggest defective MK activation in *Csk* KO and DKO mice.

Hemostatic and thrombotic defects in *Csk*/*CD148*-deficient platelets

We hypothesized that *Csk* KO mice would be predisposed to thrombosis because of increased SFK activity, rendering platelets hyperactive. To test this, we analyzed mice of all 3 genotypes in established *in vivo* models of hemostasis and thrombosis. Paradoxically, *Csk* KO mice exhibited increased bleeding in a tail injury model (Figure 2A). *CD148* KO mice exhibited normal hemostasis, whereas DKO mice had increased bleeding compared with *Csk* KO mice (Figure 2A). Increased bleeding in *Csk* KO and DKO mice could not be explained solely by reduced platelet count, which was normal in DKO mice.

To explore the kinetics of arterial thrombus formation, we employed the laser injury-induced thrombosis model in small arterioles in mice. Thrombus formation and fibrin deposition were moderately and severely reduced in *Csk* KO and DKO mice, respectively (Figure 2Bi-iv; supplemental Videos 1 and 2). Thrombus formation was also severely compromised in *CD148* KO mice, whereas fibrin deposition was only moderately reduced (Figure 2Bi-iv). Similar results were observed following FeCl₃-induced injury of the carotid artery, albeit thrombus formation was marginally better in *CD148* KO than in *Csk* KO mice (Figure 2Ci-iii; supplemental Video 3). These results demonstrate that the ability of *Csk* KO and DKO mice to form thrombi *in vivo* is markedly reduced, resulting in increased bleeding.

Aberrant platelet function underlies thrombotic and defects

To determine the cause of reduced thrombus formation observed in the different *in vivo* models, we employed the T-TAS microfluidic device, which can differentiate between platelet- and coagulation-driven defects. We found that platelets of all 3 genotypes displayed severe defects in forming stable platelet thrombi on collagen surface, as we were unable to detect an increase in the flow pressure (Figure 3Ai). However, under conditions where platelets were flowed over collagen in the presence of tissue factor to maximize coagulation, platelets of all 3 genotypes formed equally stable thrombi (Figure 3Aii), suggesting coagulation is unaltered in these mice and that defects in thrombus formation are intrinsic to platelets.

To identify specific platelet defects, we measured multiple parameters of platelet function and thrombus formation *ex vivo* at arterial shear rates on collagen I; von Willebrand factor-binding peptide (vWF-BP) and laminin; and vWF-BP, laminin, and the snake venom rhodocytin, which induces CLEC-2 signaling. Platelet deposition and thrombus formation on collagen I were markedly decreased *Csk* KO and *CD148* KO samples and further reduced in DKO samples (Figure 3Bi-iii,vi). α -Granule secretion, integrin $\alpha \text{IIb}\beta 3$ activation, and phosphatidylserine exposure (determined as P-selectin, JON/A, and Annexin V staining, respectively) followed the same trends (Figure 3Biv-iv). This likely is a consequence of markedly reduced surface levels of GPVI-FcR γ -chain, defective SFK signaling, and increased inhibitory mechanisms. We found no difference between genotypes in platelet deposition on the vWF-BP and laminin surface on which adhesion is mediated by platelet GPIIb α via immobilized plasma vWF and platelet integrin $\alpha 6\beta 1$, which binds laminin,⁴⁵ suggesting that *Csk* and *CD148* do not play major roles regulating GPIIb α or $\alpha 6\beta 1$ signaling pathways (Figure 3Bi-ii,vi). Upon complementing the vWF-BP and laminin surface with the CLEC-2 ligand rhodocytin, which drives a more robust platelet deposition,⁴⁶ adhesion

Figure 4. *Csk* and *CD148* reciprocally regulate platelet SFKs. (Ai) Representative electropherograms of capillary-based immunoassays on platelet lysates with the indicated antibodies and the quantification of peak areas ($n = 6$ mice/genotype). (Aii) Representative data from panel Ai displayed as blots. See also supplemental Figure 8. (B) Model of SFK regulation in platelets. In WT platelets, SFKs are constrained in an inactive conformation by *Csk*, which phosphorylates the C-terminal inhibitory tyrosine residue. SFKs can be activated by dephosphorylation of the inhibitory residue by *CD148*. SFKs trans-autophosphorylate each other at the activation-loop tyrosine residue and become fully active. *CD148* can also dephosphorylate the activation-loop tyrosine leading to a decrease in SFK activity. In *Csk* KO platelets, *CD148* dominates, resulting in the loss of inhibitory phosphorylation and a net increase in SFK activity. In *CD148* KO platelets, *Csk* dominates, resulting in increased inhibitory phosphorylation and markedly decreased activation-loop phosphorylation. In DKO platelets, the absence of both *Csk* and *CD148* leads to a dramatic increase in SFK activity. The differential phosphorylation of SFKs in *Csk* KO and DKO platelets supports the hypothesis of *CD148* dephosphorylating both the activation-loop and the C-terminal inhibitory tyrosine residues. Professional illustration by Patrick Lane, ScEYEnce Studios. (C) Platelet lysates were blotted for the indicated proteins. * $P < .05$, ** $P < .01$, *** $P < .001$; repeated measures 1-way ANOVA with Tukey's test; data represent mean \pm SEM.

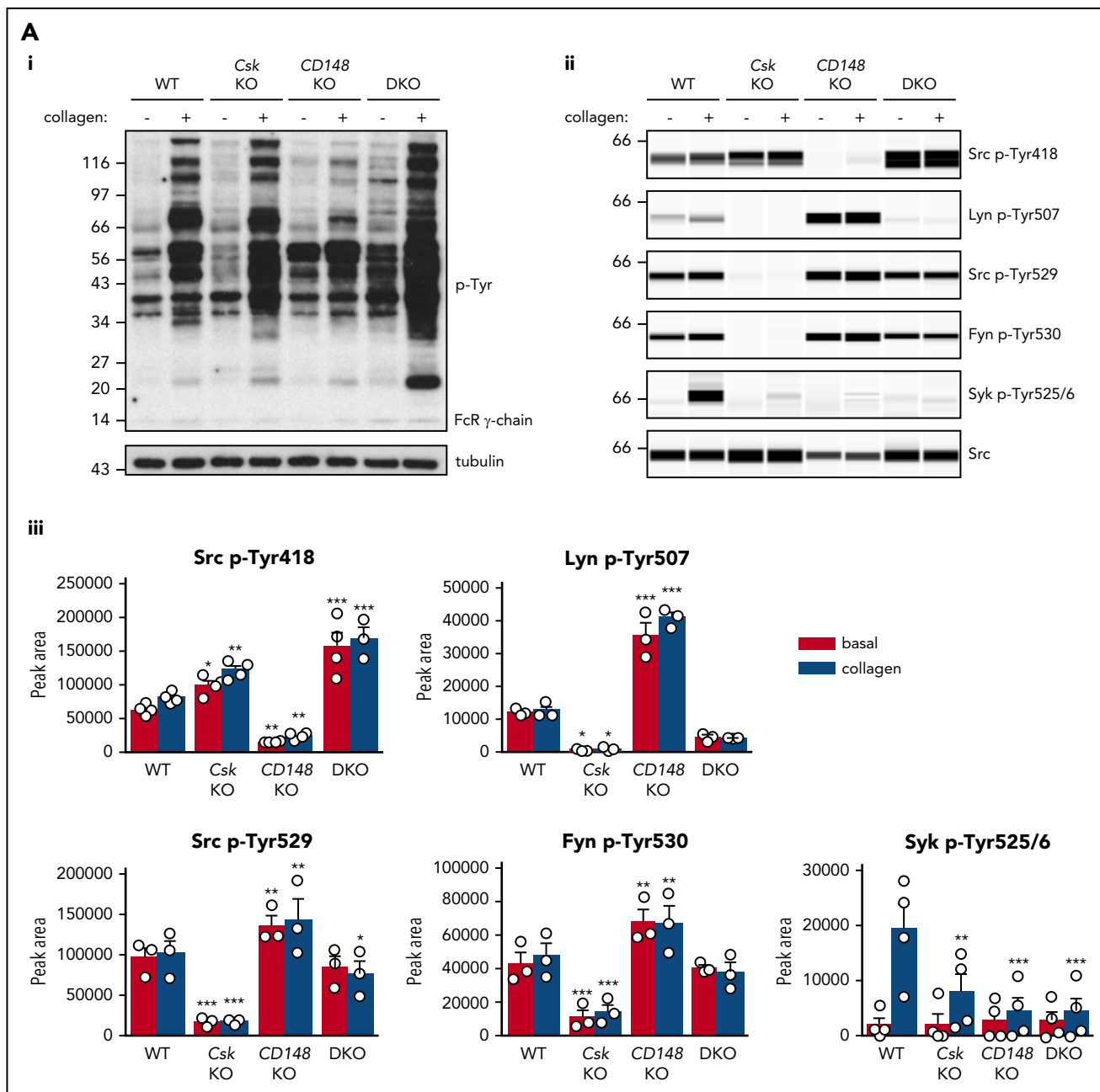
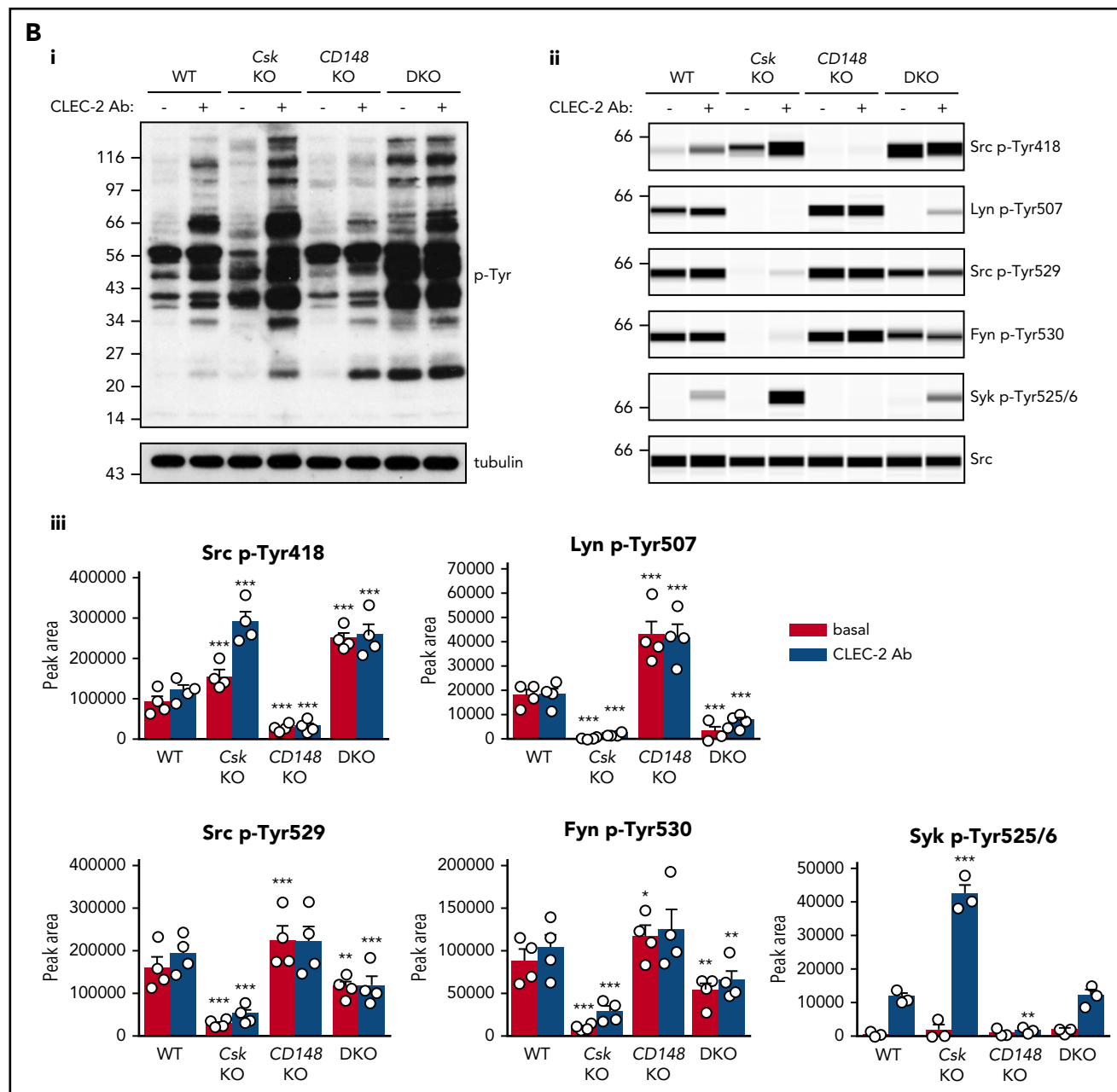


Figure 5. Csk and CD148 are critical for platelet activation signals. (Ai) Lysates of basal and collagen-stimulated (30 μ g/mL, 90 seconds) platelets were blotted for p-Tyr and tubulin. (Aii-iii) The same lysates were analyzed by capillary-based immunoassays with the indicated antibodies. Representative data displayed as blots in panel Aii. (Aiii) Quantification of peak areas from supplemental Figure 9A ($n = 3-4$ mice per genotype). See also supplemental Figure 9A. (B) Lysates of basal and CLEC-2 antibody-stimulated (10 μ g/mL, 5 minutes) platelets were analyzed as described in panels Ai-Aiii ($n = 3-4$ mice per genotype). See also supplemental Figure 9B. (C) Lysates of nonadherent (NA) and adherent (Ad) platelets from fibrinogen-coated plates (100 μ g/mL, 45 minutes, 37°C) were analyzed as described in panels Ai-Aiii. See also supplemental Figure 9C. (Civ) The same lysates were blotted for Syk p-Tyr525/6 ($n = 3-4$ mice per genotype). Differences in basal SFK activity in WT and DKO platelets in suspension (A-B) compared with nonadherent platelets (C) are due to differences in sample preparation, as demonstrated by a significant increase in Src p-Tyr418 levels in nonadherent platelets incubated on fibrinogen-coated surface (supplemental Figure 9D). (Di) Increased G6b-B phosphorylation and assembly of the G6b-B-Shp1-Shp2 complex in Csk KO and DKO platelets. Lysates of basal and collagen-stimulated (30 μ g/mL, 90 seconds) platelets were immunoprecipitated with anti-G6b-B antibody and blotted for p-Tyr, G6b-B, Shp1, and Shp2. (Dii) The role of SFKs in activating and inhibitory pathways. Once a threshold level of SFK activity is reached, ITAM, hemi-ITAM, integrin, and ITIM signaling are triggered. The kinetics and order of activation depend upon the agonist and level of SFK activity. (Dii) Professional illustration by Patrick Lane, ScEYence Studios. * $P < .05$, ** $P < .01$, *** $P < .001$; repeated-measures 2-way ANOVA with Tukey's test; data represent mean \pm SEM.

was significantly reduced in the 3 KOs (Figure 3Bi-ii,vi). Notably, CLEC-2 expression was marginally and markedly reduced in Csk KO and DKO platelets, respectively, demonstrating that Csk and CD148 participate in SFK regulation during CLEC-2-evoked hemi-ITAM signaling, as previously described.³²

We next analyzed platelets of all 3 genotypes in a range of in vitro functional assays. Consistent with previous findings, CD148 KO platelets exhibited reduced aggregation and ATP secretion to collagen and CRP stimulation, which was overcome at high concentrations of CRP (Figure 3Ci-ii). Csk KO and DKO platelets



also exhibited reduced reactivity to collagen and failed to respond to collagen-related peptide (CRP) (Figure 3Ci-ii). We also investigated the aggregation and ATP secretion response of platelets to anti-CLEC-2 antibody-mediated activation. CD148 KO platelets exhibited an increase in the lag time at low concentration of anti-CLEC-2 antibody and responded normally to a high concentration (Figure 3Ciii). In contrast, Csk KO and DKO platelets exhibited shortened lag times in response to anti-CLEC-2 antibody, despite expressing lower levels of CLEC-2 receptor (Figures 1Di-ii and 3Cii). Platelets from all 3 mouse models responded normally to thrombin and the TxA₂ analog U46619 (Figure 3Civ-v). As expected, WT platelets prepared in the absence of apyrase did not respond to 10 μ M ADP because of P2Y₁ and P2Y₁₂ receptor desensitization (Figure 3Cvi); however, Csk KO and

DKO platelets were able to aggregate and secrete ATP in response to the same concentration of ADP (Figure 4Cvi), suggesting reduced P2Y₁ and P2Y₁₂ internalization or increased signaling via these receptors, both of which use SFKs to transmit signals.² Indeed, washed platelets prepared in the presence of apyrase, preventing receptor desensitization, responded normally to 3 and 10 μ M ADP, but DKO platelets hyperresponded (Figure 3Cvii; supplemental Figure 7), supporting the hypothesis of increased P2Y₁₂ signaling.

We investigated platelet adhesion and spreading on fibrinogen, which is dependent on SFK-mediated α IIb β 3 outside-in signaling and cytoskeletal remodeling. As expected, Csk-deficient platelets spread to a greater extent than WT platelets, whereas

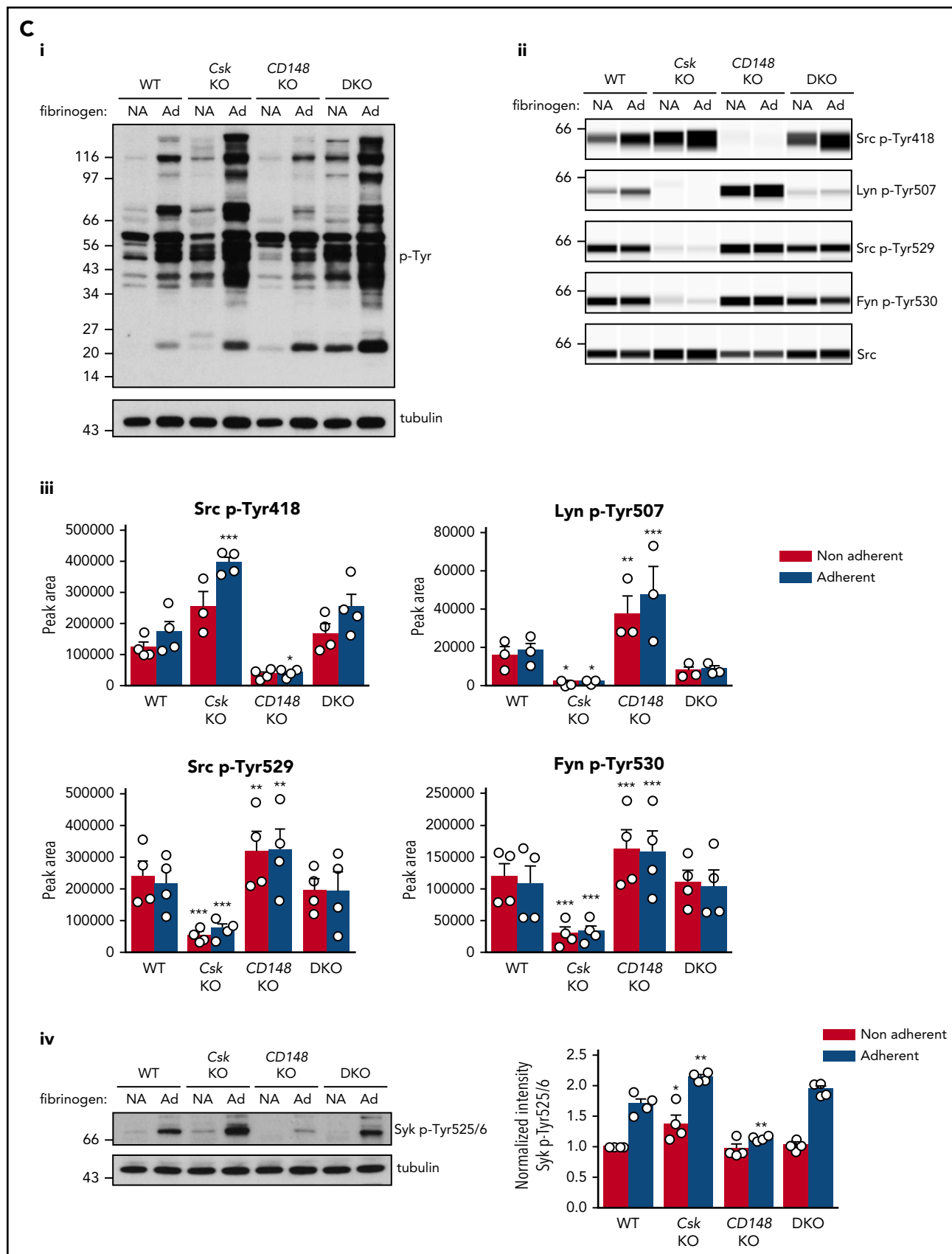
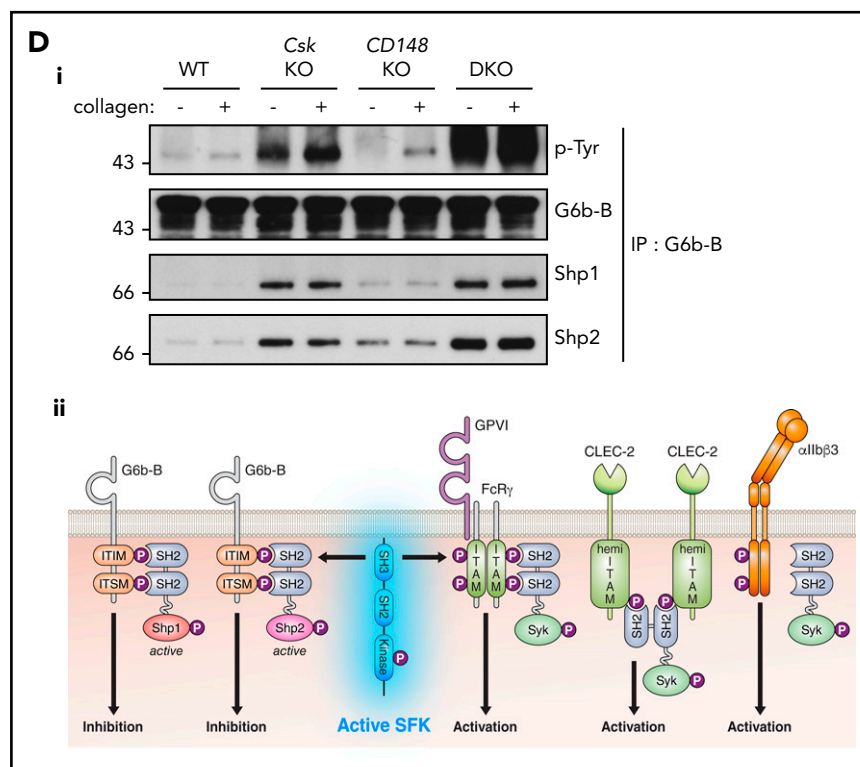


Figure 5. (Continued).

Figure 5. (Continued).



CD148-deficient platelets exhibited reduced spreading (Figure 3Di-ii). However, DKO platelets and WT platelets spread comparably, suggesting that negative feedback mechanisms were activated in DKO platelets. When platelets were preactivated with thrombin, spreading of Csk KO and DKO platelets was significantly increased compared with WT platelets (Figure 3Di-ii).

To further test the role of Csk and CD148 in α IIb β 3 signaling, we assessed clot retraction in these mice *in vitro*, revealing a significant reduction in clot retraction of CD148 KO platelets (Figure 3E). These results strongly suggest an important role for functional Src kinase activity in clot retraction.

Increased SFK activity in Csk/CD148-deficient platelets

To determine the mechanism underlying the hypothrombotic phenotypes, we assessed SFK activity in unstimulated platelets of all three genotypes. We measured *trans*-autophosphorylation of the activation loop tyrosine residue of SFKs (Src p-Tyr418) as an indirect indicator of SFK activity in resting platelets by quantitative capillary electrophoresis-based immunoassays (ProteinSimple Wes). As expected, deletion of Csk resulted in a significant increase in Src p-Tyr418, whereas deletion of CD148 resulted in a marked decrease in Src p-Tyr418 (Figure 4Ai-ii). Deletion of both Csk and CD148 resulted in an unexpected overall increase in Src p-Tyr418, demonstrating high activity SFKs in these platelets (Figure 4Ai-ii,B).

Phosphorylation of the C-terminal inhibitory tyrosine residues of Lyn (Tyr507), Src (Tyr529), and Fyn (Tyr530) is typically inversely related to SFK activity and Src p-Tyr418. Indeed, phosphorylated Lyn Tyr507 (Lyn p-Tyr507) was not detected in resting

Csk-deficient platelets (Figure 4Ai-ii), and phosphorylation of Src Tyr529 (Src p-Tyr529) and Fyn Tyr530 (Fyn p-Tyr530) were markedly decreased, suggesting that Csk is the main kinase that phosphorylates these residues and attenuates the activity of these SFKs. Conversely, phosphorylation of all three inhibitory tyrosine residues was increased in resting CD148-deficient platelets (Figure 4Ai-ii), confirming previous findings that CD148-induced dephosphorylation activates SFKs in platelets.³¹ A partial rescue of Lyn p-Tyr507, Src p-Tyr529, and Fyn p-Tyr530 was observed in DKO platelets (Figure 4Ai-ii), suggesting that in the absence of Csk and CD148, another kinase phosphorylates these residues, the obvious candidate being Chk, which was upregulated in Csk KO and DKO platelets (Figure 4C), explaining the rescue of inhibitory site phosphorylation of SFKs in DKO platelets. Expression of the tyrosine phosphatases PTP-1B, Shp1, and Shp2, all of which have been implicated in regulating SFK activity, were normal in all 3 genotypes (Figure 4C). Interestingly, SFK activity (Src p-Tyr418) was highest in DKO platelets, despite increased phosphorylation of the C-terminal inhibitory tyrosine residues of Lyn, Src, and Fyn, compared with Csk KO platelets. It remains to be determined whether phosphorylation of the activation loop and C-terminal inhibitory tyrosine residues coexist in the same molecules or in distinct pools of SFKs. Dually phosphorylated SFKs have been reported to be active in T cells.⁴⁷

We next assessed whether SFK activity in MKs is comparable to platelets. Indeed, SFKs were similarly phosphorylated in starved bone marrow-derived MKs (supplemental Figure 8A-B) as they were in resting platelets of the same genotype (Figure 4Ai-ii), compatible with increased SFK activity in Csk KO and DKO MKs and decreased SFK activity in CD148 KO MKs, which may underlie aberrant MK function and myelofibrosis in Csk KO and DKO mice.

Collectively, these findings demonstrate that Csk is an inhibitor of SFK activity in platelets and MKs. The finding that DKO platelets display markedly higher SFK activity than Csk KO platelets suggests that CD148 can act as a dual activator and inhibitor of SFK activity in platelets and MKs (Figure 4B).

ITAM and integrin receptor signaling is differentially regulated by Csk and CD148

To determine why platelets with high SFK activity were hyporeactive, we investigated tyrosine phosphorylation downstream of GPVI-FcR γ -chain, CLEC-2, and α IIb β 3, all of which rely on SFKs and Syk to initiate and propagate signaling. Because of the dramatic reduction of GPVI-FcR γ -chain expression in Csk KO and DKO platelets (Figure 1Di-ii), platelets were stimulated with a high concentration of collagen (30 μ g/mL), which signals primarily through GPVI-FcR γ -chain. Basal whole-cell tyrosine phosphorylation (p-Tyr) and Src p-Tyr418 were significantly higher in resting DKO platelets and collagen-stimulated Csk KO and DKO platelets than WT platelets (Figure 5Ai-iii; supplemental Figure 9A). In contrast, basal and collagen-mediated Src p-Tyr418 was significantly lower in CD148 KO platelets than WT platelets (Figure 5Ai-iii; supplemental Figure 9A). Induced phosphorylation of the FcR γ -chain, which is directly mediated by SFKs and acts as a docking site for Syk, was less pronounced in Csk KO and DKO platelets (Figure 5Ai) due to reduced expression of the FcR γ -chain in these platelets (Figure 1Di). Syk activation was indirectly measured as phosphorylation of Syk tyrosine residues 525 and 526 (Syk p-Tyr525/6) and correlated directly with FcR γ -chain levels and phosphorylation. Syk p-Tyr525/6 was highest in collagen-stimulated WT platelets and increased only marginally in collagen-stimulated platelets of all 3 genotypes (Figure 5Ai-iii; supplemental Figure 9A), despite Csk KO and DKO platelets having high SFK activity. These findings support a model in which receptor-mediated membrane localization of Syk is essential for activation.

Platelets were also stimulated with a high concentration of anti-CLEC-2 antibody (10 μ g/mL), mimicking podoplanin-mediated cross-linking of the receptor. The pattern and intensity of whole-cell p-Tyr and SFK phosphorylation generally mirrored that of collagen-stimulation in the various genotypes (Figure 5Bi-iii; supplemental Figure 9B). However, Syk p-Tyr525/6 was much higher in Csk KO platelets than any of the other genotypes (Figure 5Bi-iii; supplemental Figure 9B), despite reduced CLEC-2 expression. Despite the reduced CLEC-2 and GPVI-FcR γ -chain levels in DKO platelets, stimulation by anti-CLEC-2 antibody resulted in normal Syk p-Tyr525/6, whereas stimulation by collagen led to significantly reduced Syk phosphorylation, correlating with normal and reduced aggregation, respectively.

We also investigated α IIb β 3 signaling to determine the cause of increased spreading of Csk KO platelets on fibrinogen (Figure 3Di-ii). To initiate signaling, α IIb β 3 relies mainly on Src and, to a lesser extent, Fyn and is localized exclusively in nonlipid rafts.^{8,15,48,49} Whole-cell p-Tyr was increased in fibrinogen-adhered Csk KO and DKO platelets (Figure 5Ci), demonstrating a general increase in outside-in integrin signaling in these platelets. In agreement with increased spreading of Csk KO platelets but normal spreading of DKO platelets on fibrinogen (Figure 3Di-ii, basal), we found that SFK and Syk activity was increased in Csk KO platelets, but not in DKO platelets (Figure 5Cii-iv; supplemental Figure 9C).

In addition to the elevated expression of the ITIM-containing receptor G6b-B in Csk KO and DKO platelets (Figure 1Di-ii), we found a marked increase in G6b-B tyrosine phosphorylation and binding of the tyrosine phosphatases Shp1 and Shp2 under resting and collagen-stimulated conditions (Figure 5Di), suggesting increased inhibitory signaling via the G6b-B-Shp1-Shp2 complex in Csk KO and DKO platelets (Figure 5Dii). Thus, increased SFK activity in Csk KO and DKO platelets leads to compensatory upregulation of inhibitory ITIM signaling and parallel downregulation of the (hemi-)ITAM-containing GPVI-FcR γ -chain and CLEC-2 receptors, explaining the reduced activity of these platelets.

Csk is a critical inhibitor of ITAM- and integrin-mediated platelet activation

To circumvent developmental and compensatory mechanisms arising from deletion of Csk, we used a transgenic mouse model expressing a PP1-analog (3-IB-PP1)-sensitive form of Csk (Csk^{AS}), enabling rapid and specific inhibition of Csk^{AS} in these mice.³⁹ Platelet count, volume, and receptor expression were normal in Csk^{AS} mice (data not shown). Platelets from Csk^{AS} mice aggregated and secreted normally to all agonists tested in the presence of vehicle alone (dimethyl sulfoxide) (Figure 6Ai-iv) and marginally more robustly to a subthreshold concentration of anti-CLEC-2 antibody (3 μ g/mL) in the presence of 10 μ M 3-IB-PP1 (Figure 6Aiii). Inhibitor-treated Csk^{AS} platelets also spread marginally better than control on fibrinogen (Figure 6Bi-ii). Collectively, these findings validate that Csk is an inhibitor of both ITAM- and integrin receptor-mediated platelet functions. SFK activity (Src p-Tyr418) was significantly increased in resting, CRP (30 μ g/mL)-, and anti-CLEC-2 antibody (10 μ g/mL)-stimulated Csk^{AS} platelets treated with 10 μ M 3-IB-PP1 (Figure 6Ci-iii, Di-iii; supplemental Figure 10A-B). However, Lyn p-Tyr507, Src p-Tyr529, and Fyn p-Tyr530 were only minimally reduced in the presence of 3-IB-PP1 (Figure 6Cii-iii, Dii-iii; supplemental Figure 10A-B), suggesting that tyrosine phosphatases do not automatically dephosphorylate these residues in the absence of Csk. Syk activity was significantly increased at later time points after CRP stimulation (Figure 6Cii-iii; supplemental Figure 10A). Concomitantly, G6b-B was hyperphosphorylated and had more associated Shp1 and Shp2 in collagen-stimulated Csk^{AS} platelets treated with 3-IB-PP1 (Figure 6E). Because G6b-B KO platelets display markedly elevated Syk activity,²⁸ we hypothesized that the increased inhibitory signaling provided by G6b-B impeded further enhancement of CRP- and CLEC-2 antibody-mediated aggregation and overall tyrosine phosphorylation in Csk^{AS} platelets. These findings suggest that SFKs activate inhibitory pathways in parallel with activation pathways to prevent platelet hyperactivation.

Discussion

Here, we describe a fundamental mechanism controlling SFK activity in the MK lineage involving the kinase Csk and the phosphatase CD148. We show that Csk is a major inhibitor of SFKs in platelets, whereas CD148 primarily activates SFKs but also attenuates SFK activity under undefined conditions (Figures 4B and 7A). These functions of Csk and CD148 correlate with what has previously been described in immune cells.^{31,50-55} We show that lack of Csk in the MK lineage in mice results in increased SFK activity in platelets, paradoxical bleeding, and reduced thrombosis

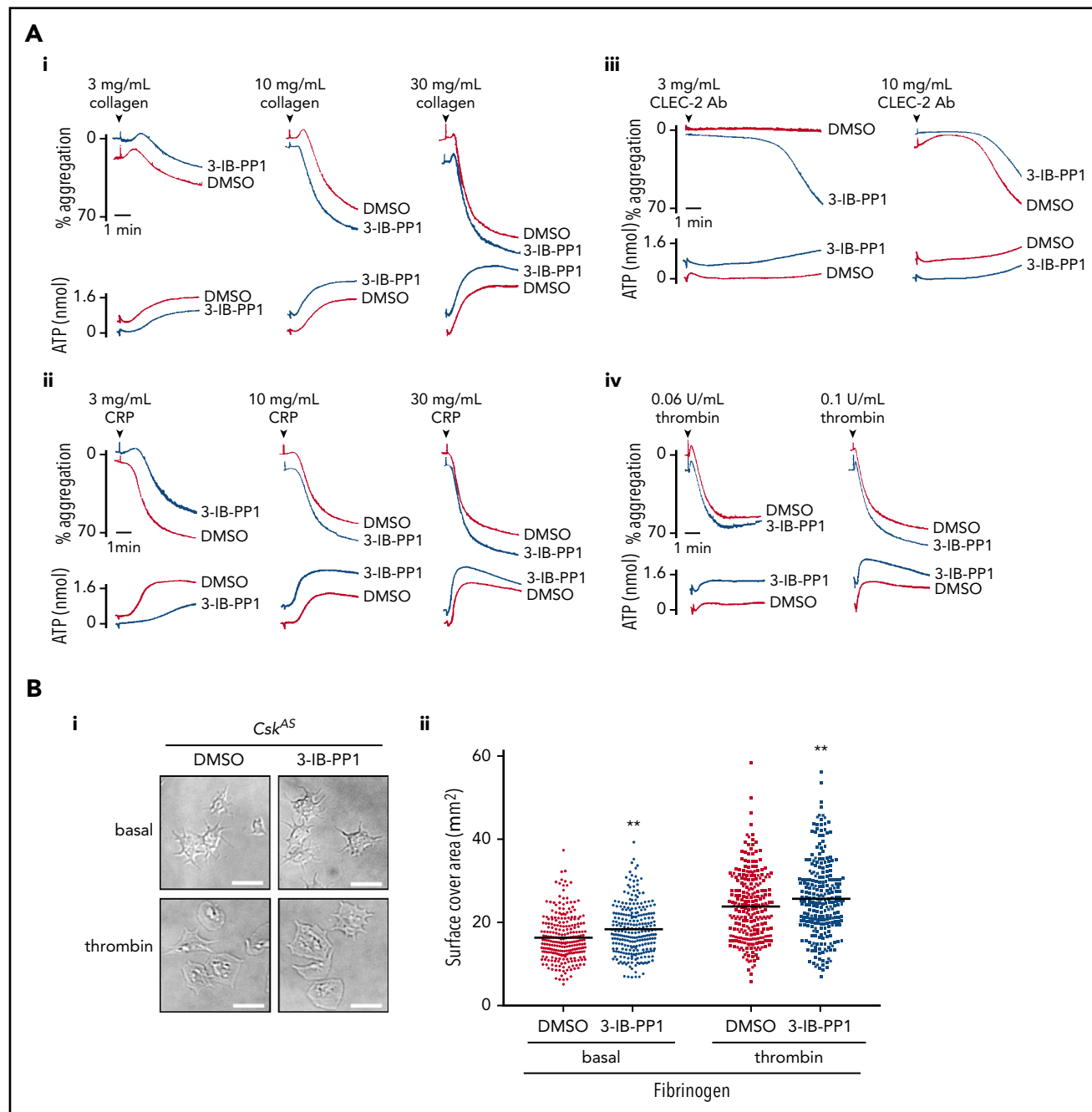


Figure 6. Csk regulates ITAM-, ITIM-, and integrin-dependent signaling in Csk^{AS} platelets. (A-E) Platelets from Csk^{AS} mice were pretreated with either dimethyl sulfoxide (DMSO) or 3-IB-PP1 (10 μ M, 10 minutes). (Ai-Aiv) Representative aggregation and ATP secretion traces of platelets from Csk^{AS} mice in response to the indicated agonists ($n = 3-4$ mice per condition per genotype). (Bi) Representative DIC microscopy images of resting (basal) and thrombin-stimulated (0.1 U/mL, 5 minutes) platelets spread on fibrinogen-coated cover-slips (100 μ g/mL, 45 minutes, 37°C; scale bar, 5 μ m). (Bii) Mean surface area of individual platelets quantified by ImageJ ($n = 256$ platelets per condition). (C-D) Lysates of platelets incubated with or without CRP (30 μ g/mL, C) or CLEC-2 antibody (10 μ g/mL, D) for the indicated times were blotted for p-Tyr and actin (Ci,Di) or analyzed by capillary-based immunoassays as described in Figure 5A (Cii-Ciii, Dii-Diii) ($n = 3-4$ mice per genotype). See also supplemental Figure 10A-B. (E) Increased G6b-B phosphorylation and assembly of the G6b-B-Shp1-Shp2 complex in collagen-stimulated Csk^{AS} platelets treated with 3-IB-PP1. Lysates of basal and collagen-stimulated (30 μ g/mL, 90 seconds) platelets were immunoprecipitated with anti-G6b-B antibody and blotted for p-Tyr, G6b-B, Shp1, and Shp2. * $P < .05$, ** $P < .01$, *** $P < .001$; ordinary (B) or repeated-measures (C-D) 2-way ANOVA with Sidak's test; data represent mean \pm SEM.

due to negative feedback mechanisms, including downregulation of (hemi-)ITAM-containing receptors and concomitant upregulation of the inhibitory ITIM-containing receptor G6b-B, rendering platelets less responsive to vascular injury (Figure 7B). In contrast, deletion of CD148 results in reduced SFK activity and

thrombus formation as a consequence of reduced (hemi-)ITAM and integrin receptor signaling. However, bleeding was normal in $CD148$ KO mice because of residual SFK activity and intact positive feedback mechanisms. Intriguingly, deletion of both Csk and $CD148$ markedly increased SFK activity, with more

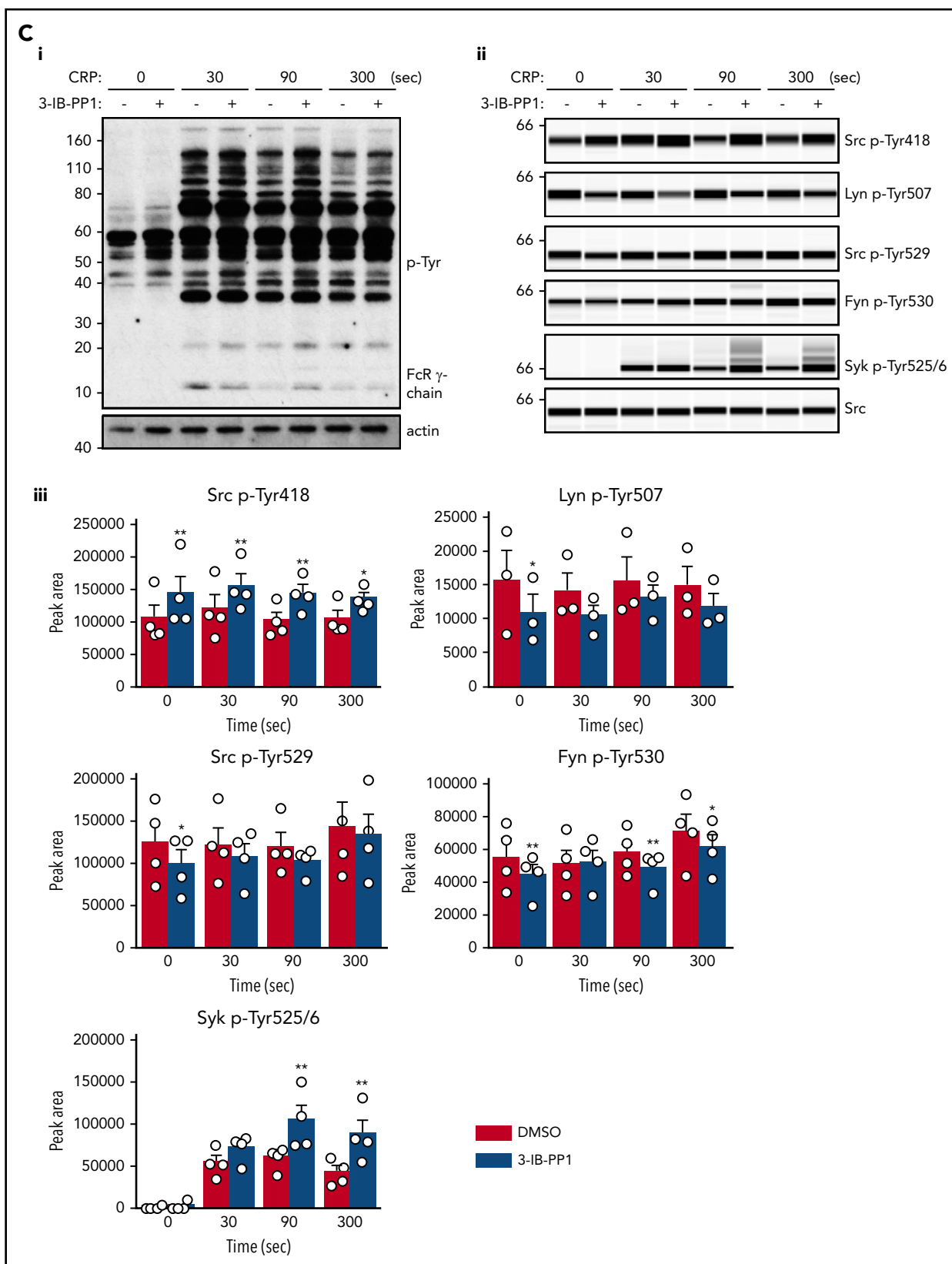


Figure 6. (Continued).

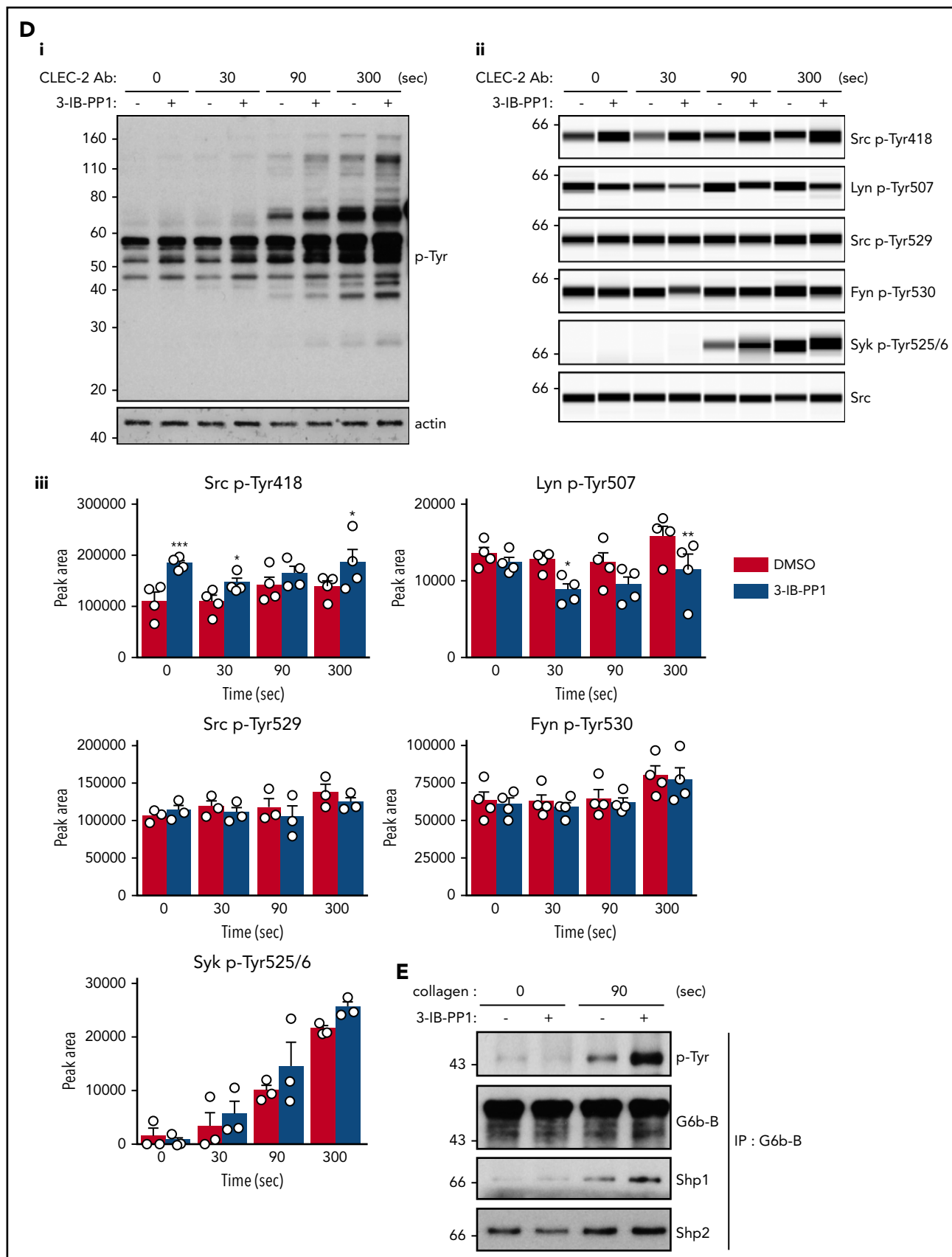


Figure 6. (Continued).

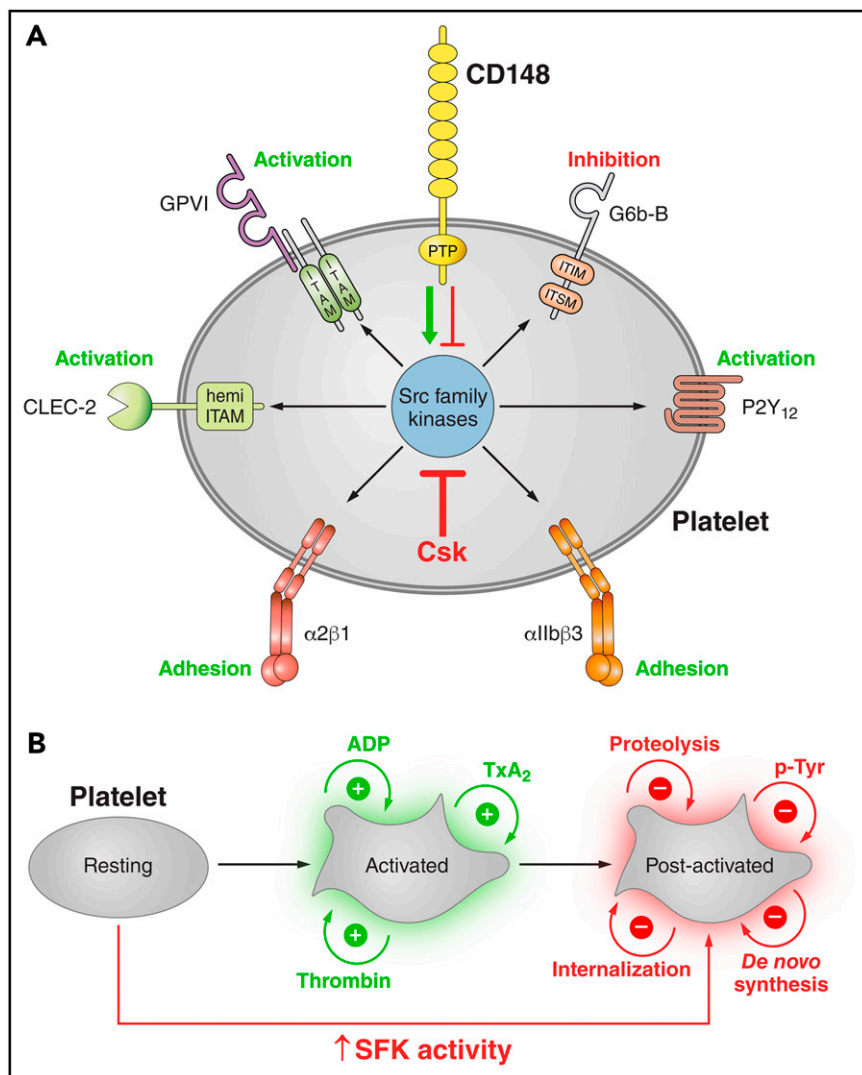


Figure 7. Regulation of platelet SFKs by the kinase Csk and the phosphatase CD148. (A) Csk and CD148 are the main regulators of SFK activity in platelets and impact different platelet signaling pathways. Csk inhibits SFK activity, whereas CD148 activates SFKs, but it can also inhibit SFK activity under conditions that have yet to be defined. In turn, SFKs regulate ITAM, hemi-ITAM, integrin, ITIM, and P2Y₁₂ receptor signaling pathways. See also Figures 4B and 5Dii. (B) Postactivated platelets. Platelets possess remarkable positive-feedback pathways (eg, ADP, TXA₂), which further enhance platelet activation. Platelet activation is followed by receptor proteolysis or internalization, de novo protein synthesis, and downregulation of tyrosine phosphorylation pathways by ITIM-containing receptors and phosphatases. Csk KO and DKO platelets have increased SFK activity, which results in reduced expression of the platelet activating receptors GPVI and CLEC-2, increased expression of the ITIM-containing receptor G6b-B, and increased ITIM signaling, suggesting that these platelets exist in a postactivated state. Professional illustration by Patrick Lane, ScEYence Studios.

pronounced bleeding and thrombotic defects than in *Csk* KO mice, because of enhanced negative feedback effects (Figure 7B). A summary of the phenotypes of *Csk* KO, *CD148* KO, and DKO mice is provided in Table 1. Thus, sustained high SFK activity in platelets does not culminate in a general increase in platelet reactivity but results in overcompensation of negative feedback mechanisms that attenuate the platelet response to various thrombogenic substrates. Moreover, the reduced platelet count in *Csk* KO mice was not due to increased platelet clearance; rather, it was a result of a reduction in platelet production, agreeing with a lack of activation and phagocytosis markers on platelets in these mice. Although mean platelet count was rescued in DKO mice, the variability in count, platelet volume, and the proportion of reticulated platelets in the circulation suggested a less robust system controlling platelet homeostasis in the absence of *Csk* and *CD148*.

Negative feedback mechanisms activated in the *Csk* KO and DKO mice, including downregulation of the (hemi-)ITAM-containing receptors GPVI-FcR γ -chain and CLEC-2 and upregulation of the ITIM-containing receptor G6b-B and tyrosine kinase Chk, likely represent cell-intrinsic adaptation of platelets to high SFK

activity. These findings are in agreement with the reduction of the ITAM-containing T-cell receptor in *Csk*-deficient T cells⁵⁶ and increased phosphorylation of the ITIM-containing receptor Sirp α , the lipid phosphatase SHIP1, and Shp1 following inhibition of *Csk*^{AS} in immune cells.⁵⁷ A plausible explanation for the downregulation of (hemi-)ITAM-containing receptors is that these receptors are direct substrates of *CD148*; similarly, the ITAM-containing T-cell receptor subunit CD3 ζ -chain is suggested to be a substrate of the tyrosine phosphatase *CD45*.^{58,59} A clear difference was observed in the downregulation of GPVI-FcR γ -chain and CLEC-2, suggesting differential regulation of these receptors. Whereas the GPVI-FcR γ -chain was severely reduced in both *Csk* KO and DKO platelets, CLEC-2 was markedly downregulated only in DKO platelets. This may be explained by the different affinities of Syk to different phospho-(hemi-)ITAMs,^{60,61} and thus the ability of the SH2 domains of Syk to protect tyrosine residues within these motifs from dephosphorylation by *CD148*, as proposed for the related kinase ZAP-70.⁶²⁻⁶⁴ We hypothesize that the higher affinity of the tandem SH2 domains of Syk for the dual phosphotyrosine residues of the FcR γ -chain ITAM in *Csk* KO platelets prevents *CD148*-mediated dephosphorylation. Sustained phosphorylation would in turn lead to internalization and degradation of the GPVI-FcR

Table 1. Summary of *Csk* KO, *CD148* KO, and DKO mouse phenotypes

Phenotype	Genotype		
	<i>Csk</i> KO	<i>CD148</i> KO	DKO
Bleeding	↑	—	↑↑
Thrombosis			
In vivo			
Laser injury	↓	↓	↓↓
FeCl ₃ injury	↓↓	↓	↓
Ex vivo			
T-TAS			
Collagen	↓	↓	↓↓
Collagen, tissue factor	—	—	—
Flow chamber			
Collagen	↓	↓	↓↓
vWF-BP, laminin, rhodocytin	↓	↓	↓
Platelet count	↓	—	—
Platelet receptors			
Expression			
GPVI-FcRγ-chain	↓↓	↓	↓↓↓
CLEC-2	↓	—	↓↓
G6b-B	↑↑	—	↑↑
Phosphorylation			
G6b-B	↑↑	—	↑↑↑
SFK activity	↑	↓	↑↑

↑, upregulated; ↓, downregulated; —, normal.

γ-chain complex. In contrast, because of the lower binding affinity of individual SH2 domains of Syk for single phosphotyrosine residues with the hemi-ITAM of CLEC-2, Syk is less capable of protecting CLEC-2 from dephosphorylation by CD148. As a consequence, less CLEC-2 is destined for degradation than FcR γ-chain in *Csk* KO platelets. However, this is not the case for DKO platelets, where no CD148 is present to dephosphorylate CLEC-2; hence, it is markedly downregulated. Further work is needed to validate this hypothesis.

Analysis of tyrosine phosphorylation downstream of GPVI, CLEC-2, and αIIbβ3 revealed that activation of Syk is dependent not only on SFK activity but also on the presence of appropriate docking sites at the plasma membrane, providing evidence that increased SFK activity alone is insufficient to initiate downstream signaling. A growing body of evidence has established G6b-B as a major inhibitor of (hemi-)ITAM-containing receptor signaling in platelets, acting primarily at the level of Syk.^{28,65} It is therefore likely that increased G6b-B expression, phosphorylation, and Shp1 and Shp2 association contributes to the attenuation of (hemi-)ITAM signaling in *Csk* KO and DKO platelets. Upregulation of Chk in the absence of *Csk* likely also contributes to the attenuation of SFK-mediated signaling in these platelets, albeit less efficiently than its structurally related counterpart, *Csk*. Although, Chk was previously reported in platelets,⁶⁶ it was not detected in either human or mouse platelets by mass spectrometry,^{3,4} in

agreement with our findings from WT platelets. Thus, the combination of reduced (hemi-)ITAM-containing receptor expression combined with increased ITIM-containing receptor and Chk expression result in a reduction in platelet reactivity to specific substrates. This is better tolerated than preactivated platelets that can trigger disseminated intravascular coagulation and death.

To circumvent masking effects of negative feedback mechanisms in *Csk* KO or DKO mice, we used *Csk*^{AS} mice. Inhibition of *Csk*^{AS} in platelets from these mice resulted in significantly reduced phosphorylation of the C-terminal inhibitory tyrosine residues of SFKs and increased SFK and Syk activity, similar to that reported in immune cells.^{39,57,67} However, inhibition of *Csk*^{AS} in platelets failed to have an effect on platelet aggregation. This can be partially explained by increased formation of the G6b-B-Shp1-Shp2 complex, counteracting the effect of increased SFK activity on Syk activation.^{25,28} Our findings also suggest that *Csk* plays little role in attenuating GPVI and CLEC-2 signaling once initiated, mainly providing a break prior to ligand engagement and receptor clustering to prevent unwanted signaling by the receptors. However, this was not the case for αIIbβ3-mediated platelet spreading on fibrinogen, which was enhanced either in the absence of *Csk* or following inhibition of *Csk*^{AS}, suggesting *Csk* differentially regulates integrin and ITAM-containing receptor signaling. Previous work from our group suggests that G6b-B facilitates rather than inhibits integrin-mediated responses in platelets and MKs²⁸; thus, upregulation of the G6b-B-Shp1-Shp2 complex is predicted to enhance rather than attenuate platelet spreading, as observed.

In addition to filling a major gap in our knowledge of how SFKs are regulated in the MK lineage, findings from this study are also clinically relevant, demonstrating for the first time that either increased or decreased platelet SFK activity can lead to reduced thrombus formation and bleeding. Our study highlights, that loss of an inhibitor of platelet activation, such as *Csk*, can lead to paradoxical bleeding due to the robust negative feedback mechanisms that get activated. This may provide important mechanistic insights into the phenomenon of early platelet dysfunction observed in severe trauma patients displaying “exhausted” platelets,⁶⁸ showing reduced thrombus formation on collagen.⁶⁹ Our findings suggest that platelets in the circulation can undergo cell-intrinsic changes, leading to downregulation of activation pathways and upregulation of inhibitory mechanisms, which may contribute to platelet dysfunction in trauma patients. Moreover, certain tyrosine kinase inhibitors used to treat cancer patients inhibit SFKs or *Csk* and are accompanied by bleeding side effects. Accordingly, the increased bleeding risk associated with use of the Bcr-Abl inhibitor dasatinib is ascribed to its off-target effects on platelet SFKs.^{70,71} Similarly, bleeding side effects of the Btk inhibitor ibrutinib may be partially explained by its potent off-target effect on *Csk*.^{72,73} Based on our findings, CD148 is an attractive antithrombotic drug target, and its inhibition should attenuate, but not completely block, the main platelet activation pathways and have minimal bleeding side effects. Tyrosine phosphatases are increasingly considered to be druggable,⁷⁴ which is supported by the recent development of the highly specific Shp2 inhibitor SHP099⁷⁵; thus, targeting CD148 is not inconceivable.

Acknowledgments

The authors thank Timo Vögtle for critical reading of the manuscript and invaluable discussions, Quadratech Diagnostics for providing the T-TAS device, and all members of the Birmingham Biomedical Sciences Unit for maintenance of mouse colonies.

J.M. and Z.N. are British Heart Foundation (BHF) postdoctoral research associates. A.M. is a BHF Intermediate Basic Science Research Fellow (FS/15/58/31784), and Y.A.S. is a BHF Senior Basic Science Research Fellow (FS/13/1/29894). R.A.G. was supported by the government of the Sultanate of Oman. This work was supported by BHF project grant PG/11/108/29237 and program grant RG/15/13/31673.

Authorship

Contribution: J.M., Z.N., A.M., and Y.A.S. contributed to conceptualization; J.M., Z.N., J.W.M.H., A.M., and Y.A.S. contributed to methodology; J.M., Z.N., C.W.S., R.A.G., J.P.v.G., B.M.E.T., G.E.J., A.M., and Y.A.S. contributed to formal analysis; J.M., Z.N., G.D.N., C.W.S., M.J.G., R.A.G., J.P.v.G., S.H., L.B., J.N.C., L.T., M.J.E.K., P.H., J.W.M.H., A.M., and Y.A.S. contributed to investigation; Y.A.S. contributed resources; A.T. and A.W. contributed mouse models and reagents; P.H. contributed equipment and expertise; J.M., Z.N., A.M., and Y.A.S. wrote the manuscript; J.M., Z.N., J.W.M.H., G.E.J., A.W., A.M., and Y.A.S. revised and edited the manuscript; and A.M. and Y.A.S. supervised the study.

Conflict-of-interest disclosure: The authors declare no competing financial interests.

ORCID profiles: J.M., 0000-0002-6212-1604; Z.N., 0000-0001-6517-2071; M.J.G., 0000-0003-1457-987X; L.B., 0000-0002-6327-7117; J.N.C., 0000-0002-4376-978X; M.J.E.K., 0000-0001-8987-6532; P.H., 0000-0003-4610-8909; G.E.J., 0000-0003-4362-1133; A.W., 0000-0002-2414-9024; A.M., 0000-0002-0204-3325; Y.A.S., 0000-0002-0947-9957.

Correspondence: Yotis A. Senis, Institute of Cardiovascular Sciences, College of Medical and Dental Sciences, University of Birmingham, Birmingham B15 2TT, United Kingdom; e-mail: y.senis@bham.ac.uk.

Footnotes

Submitted 9 February 2017; accepted 23 December 2017. Prepublished online as *Blood* First Edition paper, 4 January 2018; DOI 10.1182/blood-2017-02-768077.

*J.M. and Z.N. contributed equally to this study.

The online version of this article contains a data supplement.

There is a *Blood* Commentary on this article in this issue.

The publication costs of this article were defrayed in part by page charge payment. Therefore, and solely to indicate this fact, this article is hereby marked "advertisement" in accordance with 18 USC section 1734.

REFERENCES

1. Golden A, Nemeth SP, Brugge JS. Blood platelets express high levels of the pp60c-src-specific tyrosine kinase activity. *Proc Natl Acad Sci USA*. 1986;83(4):852-856.
2. Senis YA, Mazharian A, Mori J. Src family kinases: at the forefront of platelet activation. *Blood*. 2014;124(13):2013-2024.
3. Burkhardt JM, Vaudel M, Gambaryan S, et al. The first comprehensive and quantitative analysis of human platelet protein composition allows the comparative analysis of structural and functional pathways. *Blood*. 2012;120(15):e73-e82.
4. Zeiler M, Moser M, Mann M. Copy number analysis of the murine platelet proteome spanning the complete abundance range. *Mol Cell Proteomics*. 2014;13(12):3435-3445.
5. Ezumi Y, Shindoh K, Tsuji M, Takayama H. Physical and functional association of the Src family kinases Fyn and Lyn with the collagen receptor glycoprotein VI-Fc receptor gamma chain complex on human platelets. *J Exp Med*. 1998;188(2):267-276.
6. Quek LS, Pasquet JM, Hers I, et al. Fyn and Lyn phosphorylate the Fc receptor gamma chain downstream of glycoprotein VI in murine platelets, and Lyn regulates a novel feedback pathway. *Blood*. 2000;96(13):4246-4253.
7. Arias-Salgado EG, Lizano S, Sarkar S, Brugge JS, Ginsberg MH, Shattil SJ. Src kinase activation by direct interaction with the integrin beta cytoplasmic domain. *Proc Natl Acad Sci USA*. 2003;100(23):13298-13302.
8. Reddy KB, Smith DM, Plow EF. Analysis of Fyn function in hemostasis and alphaIIb beta3-integrin signaling. *J Cell Sci*. 2008;121(Pt 10):1641-1648.
9. Schmaier AA, Zou Z, Kazlauskas A, et al. Molecular priming of Lyn by GPVI enables an immune receptor to adopt a hemostatic role. *Proc Natl Acad Sci USA*. 2009;106(50):21167-21172.
10. Maxwell MJ, Yuan Y, Anderson KE, Hibbs ML, Salem HH, Jackson SP. SHP1 and Lyn Kinase Negatively Regulate Integrin alpha IIb beta 3 signaling in platelets. *J Biol Chem*. 2004;279(31):32196-32204.
11. Falati S, Edmead CE, Poole AW. Glycoprotein IIb-V-IX, a receptor for von Willebrand factor, couples physically and functionally to the Fc receptor gamma-chain, Fyn, and Lyn to activate human platelets. *Blood*. 1999;94(5):1648-1656.
12. Ozaki Y, Asazuma N, Suzuki-Inoue K, Berndt MC. Platelet GPIIb-IX-V-dependent signaling. *J Thromb Haemost*. 2005;3(8):1745-1751.
13. Suzuki-Inoue K, Tulasne D, Shen Y, et al. Association of Fyn and Lyn with the proline-rich domain of glycoprotein VI regulates intracellular signaling. *J Biol Chem*. 2002;277(24):21561-21566.
14. Fox JE, Lipfert L, Clark EA, Reynolds CC, Austin CD, Brugge JS. On the role of the platelet membrane skeleton in mediating signal transduction. Association of GP IIb-IIIa, pp60c-src, pp62c-yes, and the p21ras GTPase-activating protein with the membrane skeleton. *J Biol Chem*. 1993;268(34):25973-25984.
15. Oberfell A, Eto K, Mocsai A, et al. Coordinate interactions of Csk, Src, and Syk kinases with [alpha]IIb[beta]3 initiate integrin signaling to the cytoskeleton. *J Cell Biol*. 2002;157(2):265-275.
16. Murugappan S, Shankar H, Bhamidipati S, Dorsam RT, Jin J, Kunapuli SP. Molecular mechanism and functional implications of thrombin-mediated tyrosine phosphorylation of PKCdelta in platelets. *Blood*. 2005;106(2):550-557.
17. Li Z, Zhang G, Liu J, et al. An important role of the SRC family kinase Lyn in stimulating platelet granule secretion. *J Biol Chem*. 2010;285(17):12559-12570.
18. Kim S, Kunapuli SP. Negative regulation of Gq-mediated pathways in platelets by G(12/13) pathways through Fyn kinase. *J Biol Chem*. 2011;286(27):24170-24179.
19. Xiang B, Zhang G, Stefanini L, et al. The Src family kinases and protein kinase C synergize to mediate Gq-dependent platelet activation. *J Biol Chem*. 2012;287(49):41277-41287.
20. Hardy AR, Jones ML, Mundell SJ, Poole AW. Reciprocal cross-talk between P2Y1 and P2Y12 receptors at the level of calcium signaling in human platelets. *Blood*. 2004;104(6):1745-1752.
21. Nash CA, Séverin S, Dawood BB, et al. Src family kinases are essential for primary aggregation by G(i)-coupled receptors. *J Thromb Haemost*. 2010;8(10):2273-2282.
22. Poole A, Gibbins JM, Turner M, et al. The Fc receptor gamma-chain and the tyrosine kinase Syk are essential for activation of mouse platelets by collagen. *EMBO J*. 1997;16(9):2333-2341.
23. Coxon CH, Geer MJ, Senis YA. ITIM receptors: more than just inhibitors of platelet activation. *Blood*. 2017;129(26):3407-3418.
24. Hua CT, Gamble JR, Vadas MA, Jackson DE. Recruitment and activation of SHP-1 protein-tyrosine phosphatase by human platelet endothelial cell adhesion molecule-1 (PECAM-1). Identification of immunoreceptor tyrosine-based inhibitory motif-like binding motifs and substrates. *J Biol Chem*. 1998;273(43):28332-28340.
25. Mazharian A, Mori J, Wang YJ, et al. Megakaryocyte-specific deletion of the protein-tyrosine phosphatases Shp1 and Shp2 causes abnormal megakaryocyte

- development, platelet production, and function. *Blood*. 2013;121(20):4205-4220.
26. Jackson DE, Ward CM, Wang R, Newman PJ. The protein-tyrosine phosphatase SHP-2 binds platelet/endothelial cell adhesion molecule-1 (PECAM-1) and forms a distinct signaling complex during platelet aggregation. Evidence for a mechanistic link between PECAM-1- and integrin-mediated cellular signaling. *J Biol Chem*. 1997;272(11):6986-6993.
 27. Falati S, Patil S, Gross PL, et al. Platelet PECAM-1 inhibits thrombus formation in vivo. *Blood*. 2006;107(2):535-541.
 28. Mazharian A, Wang YJ, Mori J, et al. Mice lacking the ITIM-containing receptor G6b-B exhibit macrothrombocytopenia and aberrant platelet function. *Sci Signal*. 2012;5(248):ra78.
 29. Hermiston ML, Xu Z, Weiss A. CD45: a critical regulator of signaling thresholds in immune cells. *Annu Rev Immunol*. 2003;21(1):107-137.
 30. Senis YA, Tomlinson MG, Ellison S, et al. The tyrosine phosphatase CD148 is an essential positive regulator of platelet activation and thrombosis. *Blood*. 2009;113(20):4942-4954.
 31. Ellison S, Mori J, Barr AJ, Senis YA. CD148 enhances platelet responsiveness to collagen by maintaining a pool of active Src family kinases. *J Thromb Haemost*. 2010;8(7):1575-1583.
 32. Mori J, Wang YJ, Ellison S, et al. Dominant role of the protein-tyrosine phosphatase CD148 in regulating platelet activation relative to protein-tyrosine phosphatase-1B. *Arterioscler Thromb Vasc Biol*. 2012;32(12):2956-2965.
 33. Roskoski R Jr. Src kinase regulation by phosphorylation and dephosphorylation. *Biochem Biophys Res Commun*. 2005;331(1):1-14.
 34. Nada S, Okada M, MacAuley A, Cooper JA, Nakagawa H. Cloning of a complementary DNA for a protein-tyrosine kinase that specifically phosphorylates a negative regulatory site of p60c-src. *Nature*. 1991;351(6321):69-72.
 35. Davidson D, Chow LM, Veillette A. Chk, a Csk family tyrosine protein kinase, exhibits Csk-like activity in fibroblasts, but not in an antigen-specific T-cell line. *J Biol Chem*. 1997;272(2):1355-1362.
 36. Schmedt C, Saijo K, Niidome T, Kühn R, Aizawa S, Tarakhovskiy A. Csk controls antigen receptor-mediated development and selection of T-lineage cells. *Nature*. 1998;394(6696):901-904.
 37. Katsumoto TR, Kudo M, Chen C, et al. The phosphatase CD148 promotes airway hyper-responsiveness through SRC family kinases. *J Clin Invest*. 2013;123(5):2037-2048.
 38. Tiedt R, Schomber T, Hao-Shen H, Skoda RC. Pf4-Cre transgenic mice allow the generation of lineage-restricted gene knockouts for studying megakaryocyte and platelet function in vivo. *Blood*. 2007;109(4):1503-1506.
 39. Tan YX, Manz BN, Freedman TS, Zhang C, Shokat KM, Weiss A. Inhibition of the kinase Csk in thymocytes reveals a requirement for actin remodeling in the initiation of full TCR signaling. *Nat Immunol*. 2014;15(2):186-194.
 40. Pearce AC, Senis YA, Billadeau DD, Turner M, Watson SP, Vigorito E. Vav1 and vav3 have critical but redundant roles in mediating platelet activation by collagen. *J Biol Chem*. 2004;279(52):53955-53962.
 41. Ohlmann P, Eckly A, Freund M, Cazenave JP, Offermanns S, Gachet C. ADP induces partial platelet aggregation without shape change and potentiates collagen-induced aggregation in the absence of Gα₁₂. *Blood*. 2000;96(6):2134-2139.
 42. Smith CW, Thomas SG, Raslan Z, et al. Mice lacking the inhibitory collagen receptor LAIR-1 exhibit a mild thrombocytosis and hyperactive platelets. *Arterioscler Thromb Vasc Biol*. 2017;37(5):823-835.
 43. Pertuy F, Aguilar A, Strassel C, et al. Broader expression of the mouse platelet factor 4-cre transgene beyond the megakaryocyte lineage. *J Thromb Haemost*. 2015;13(1):115-125.
 44. Spangrude GJ, Lewandowski D, Martelli F, et al. P-selectin sustains extramedullary hematopoiesis in the Gata1 low model of myelofibrosis. *Stem Cells*. 2016;34(1):67-82.
 45. Schaff M, Tang C, Maurer E, et al. Integrin α₆β1 is the main receptor for vascular laminins and plays a role in platelet adhesion, activation, and arterial thrombosis. *Circulation*. 2013;128(5):541-552.
 46. de Witt SM, Swieringa F, Cavill R, et al. Identification of platelet function defects by multi-parameter assessment of thrombus formation. *Nat Commun*. 2014;5:4257.
 47. Nika K, Soldani C, Salek M, et al. Constitutively active Lck kinase in T cells drives antigen receptor signal transduction. *Immunity*. 2010;32(6):766-777.
 48. Séverin S, Nash CA, Mori J, et al. Distinct and overlapping functional roles of Src family kinases in mouse platelets. *J Thromb Haemost*. 2012;10(8):1631-1645.
 49. Arias-Salgado EG, Lizano S, Shattil SJ, Ginsberg MH. Specification of the direction of adhesive signaling by the integrin beta cytoplasmic domain. *J Biol Chem*. 2005;280(33):29699-29707.
 50. Pera IL, Iuliano R, Florio T, et al. The rat tyrosine phosphatase eta increases cell adhesion by activating c-Src through dephosphorylation of its inhibitory phosphotyrosine residue. *Oncogene*. 2005;24(19):3187-3195.
 51. Stepanek O, Kalina T, Draber P, et al. Regulation of Src family kinases involved in T cell receptor signaling by protein-tyrosine phosphatase CD148. *J Biol Chem*. 2011;286(25):22101-22112.
 52. McNeill L, Salmond RJ, Cooper JC, et al. The differential regulation of Lck kinase phosphorylation sites by CD45 is critical for T cell receptor signaling responses. *Immunity*. 2007;27(3):425-437.
 53. Zikherman J, Jenne C, Watson S, et al. CD45-Csk phosphatase-kinase titration uncouples basal and inducible T cell receptor signaling during thymic development. *Immunity*. 2010;32(3):342-354.
 54. Lin J, Weiss A. The tyrosine phosphatase CD148 is excluded from the immunologic synapse and down-regulates prolonged T cell signaling. *J Cell Biol*. 2003;162(4):673-682.
 55. Davis SJ, van der Merwe PA. The kinetic segregation model: TCR triggering and beyond. *Nat Immunol*. 2006;7(8):803-809.
 56. Schmedt C, Tarakhovskiy A. Autonomous maturation of alpha/beta T lineage cells in the absence of COOH-terminal Src kinase (Csk). *J Exp Med*. 2001;193(7):815-826.
 57. Freedman TS, Tan YX, Skrzypczynska KM, et al. LynA regulates an inflammation-sensitive signaling checkpoint in macrophages. *eLife*. 2015;4:4.
 58. Furukawa T, Itoh M, Krueger NX, Streuli M, Saito H. Specific interaction of the CD45 protein-tyrosine phosphatase with tyrosine-phosphorylated CD3 zeta chain. *Proc Natl Acad Sci USA*. 1994;91(23):10928-10932.
 59. Kashio N, Matsumoto W, Parker S, Rothstein DM. The second domain of the CD45 protein tyrosine phosphatase is critical for interleukin-2 secretion and substrate recruitment of TCR-zeta in vivo. *J Biol Chem*. 1998;273(50):33856-33863.
 60. Isakov N, Wange RL, Burgess WH, Watts JD, Aebersold R, Samelson LE. ZAP-70 binding specificity to T cell receptor tyrosine-based activation motifs: the tandem SH2 domains of ZAP-70 bind distinct tyrosine-based activation motifs with varying affinity. *J Exp Med*. 1995;181(1):375-380.
 61. Ottinger EA, Botfield MC, Shoelson SE. Tandem SH2 domains confer high specificity in tyrosine kinase signaling. *J Biol Chem*. 1998;273(2):729-735.
 62. Iwashima M, Irving BA, van Oers NS, Chan AC, Weiss A. Sequential interactions of the TCR with two distinct cytoplasmic tyrosine kinases. *Science*. 1994;263(5150):1136-1139.
 63. Ashe JM, Wiest DL, Abe R, Singer A. ZAP-70 protein promotes tyrosine phosphorylation of T cell receptor signaling motifs (ITAMs) in immature CD4(+)8(+) thymocytes with limiting p56(lck). *J Exp Med*. 1999;189(7):1163-1168.
 64. Qian D, Mollenauer MN, Weiss A. Dominant-negative zeta-associated protein 70 inhibits T cell antigen receptor signaling. *J Exp Med*. 1996;183(2):611-620.
 65. Coxon CH, Sadler AJ, Huo J, Campbell RD. An investigation of hierarchical protein recruitment to the inhibitory platelet receptor, G6B-b. *PLoS One*. 2012;7(11):e49543.
 66. Hirao A, Hamaguchi I, Suda T, Yamaguchi N. Translocation of the Csk homologous kinase (Chk/Hyl) controls activity of CD36-anchored Lyn tyrosine kinase in thrombin-stimulated platelets. *EMBO J*. 1997;16(9):2342-2351.
 67. Manz BN, Tan YX, Courtney AH, et al. Small molecule inhibition of Csk alters affinity recognition by T cells. *eLife*. 2015;4:4.
 68. Wohlaue MV, Moore EE, Thomas S, et al. Early platelet dysfunction: an unrecognized role in the acute coagulopathy of trauma. *J Am Coll Surg*. 2012;214(5):739-746.
 69. Li R, Elmongy H, Sims C, Diamond SL. Ex vivo recapitulation of trauma-induced coagulopathy and preliminary assessment of trauma patient platelet function under flow

- using microfluidic technology. *J Trauma Acute Care Surg*. 2016;80(3):440-449.
70. Quintás-Cardama A, Han X, Kantarjian H, Cortes J. Tyrosine kinase inhibitor-induced platelet dysfunction in patients with chronic myeloid leukemia. *Blood*. 2009;114(2):261-263.
71. Gratapac MP, Martin V, Valéra MC, et al. The new tyrosine-kinase inhibitor and anticancer drug dasatinib reversibly affects platelet activation in vitro and in vivo. *Blood*. 2009;114(9):1884-1892.
72. Levade M, David E, Garcia C, et al. Ibrutinib treatment affects collagen and von Willebrand factor-dependent platelet functions. *Blood*. 2014;124(26):3991-3995.
73. Honigberg LA, Smith AM, Sirisawad M, et al. The Bruton tyrosine kinase inhibitor PCI-32765 blocks B-cell activation and is efficacious in models of autoimmune disease and B-cell malignancy. *Proc Natl Acad Sci USA*. 2010;107(29):13075-13080.
74. Tautz L, Senis YA, Oury C, Rahmouni S. Perspective: Tyrosine phosphatases as novel targets for antiplatelet therapy. *Bioorg Med Chem*. 2015;23(12):2786-2797.
75. Chen YN, LaMarche MJ, Chan HM, et al. Allosteric inhibition of SHP2 phosphatase inhibits cancers driven by receptor tyrosine kinases. *Nature*. 2016;535(7610):148-152.
76. Nieminen PLH, Vähäkangas K, Huusko A, Rautio A. Standardised regression coefficient as an effect size index in summarising findings in epidemiological studies. *Epidemiol Biostat Public Health*. 2013;10(4):e8854.